3-14-2014

Ultraviolet Light Emitting Diode Optical Power Characterization

Christopher S. Bates

ULTRAVIOLET LIGHT EMITTING DIODE OPTICAL POWER CHARACTERIZATION

THESIS

Christopher S. Bates, Captain, USAF, BSC

AFIT-ENV-14-M-07

DEPARTMENT OF THE AIR FORCE
AIR UNIVERSITY

AIR FORCE INSTITUTE OF TECHNOLOGY

Wright-Patterson Air Force Base, Ohio

AFIT-ENV-14-M-07

ULTRAVIOLET LIGHT EMITTING DIODE OPTICAL POWER CHARACTERIZATION

THESIS

Presented to the Faculty

Department of Systems Engineering and Management

Graduate School of Engineering and Management

Air Force Institute of Technology

Air University

Air Education and Training Command

In Partial Fulfillment of the Requirements for the

Degree of Master of Science in Industrial Hygiene Engineering and Science

Christopher S. Bates, MS

Captain, USAF, BSC

March 2014

AFIT-ENV-14-M-07

ULTRAVIOLET LIGHT EMITTING DIODE OPTICAL POWER CHARACTERIZATION

Christopher S. Bates, BSC, MS

Captain, USAF

Approved:

//Signed//	14 Mar 14
Michael E. Miller, Ph.D. (Chairman)	Date
//Signed//	14 Mar 14
Dirk P. Yamamoto, Lt Col, USAF, Ph.D., BSC (Member)	Date
//Signed//	14 Mar 14
LeeAnn Racz, Lt Col, USAF, Ph.D., BSC (Member)	Date
//Signed//	14 Mar 14
Michael R. Grimaila, Ph.D., CISM, CISSP (Member)	Date

Abstract

Obtaining a cost effective way to produce safe drinking water is not only a priority of almost every residential community in the United States, but the Department of Defense has a specific interest cutting edge technology in this domain for disinfecting water in a foreign nation during a war campaign. The development of ultraviolet (UV) Light Emitting Diode (LED) technology is a potentially important step towards being able to conduct this kind of disinfection with fewer resources. The traditional UV source in use for disinfection today is the mercury lamp. This UV source requires high amounts of voltage, requires significant periods of time for warming up, and is not typically lightweight enough or versatile enough to be useful in a deployed setting.

This project is intended to characterize the optical power for various short wavelength UV LEDs. This optical power is important in determining how much current is needed to deactivate bacteria and other pathogens or to optimize hydroxyl radical production to oxidize compounds in water.

The results from this study indicate there is a linear relationship between optical power and current for air measurements. The data collected in this research were applied to characterize the performance of LEDs for the two tandem projects and building a model to optimize the design and performance of UV LED based reactors. Additionally, this research attempted to measure UV LED emission in water. Issues associated with these measurements are discussed.

Acknowledgments

I am thankful for my thesis advisor, Dr. Michael E. Miller, for his time, endless patience, and encouragement as he carved the path for my research effort. Without his guidance, I would likely never have figured out how to make the different experiments work and certainly not grasp the importance of this characterization. My appreciation also goes to Dr. Michael R. Grimaila and Dr. LeAnn Racz for their assistance in purchasing the necessary items, assisting with troubleshooting, and guidance. I am also thankful for all of the assistance Dr. Daniel L. Felker's expertise with the lab and the DASYLAB software, which was critical for this research effort.

Christopher S. Bates

Table of Contents

Page

List of Figures

Page

List of Tables

Page

I. Introduction

General Background

LEDs are used in multiple applications in today's society. A few examples would be in the auto industry in tail lights, headlights, and dash lights (Lenk and Lenk, 2010). More specifically, UV LEDs have been utilized in chemical recognition equipment, such as high performance liquid chromatography (HPLC) (Phytosafe, 2013). The HPLC uses UV detectors to analyze radiation absorbance to identify chemicals of concern, such as carcinogenic agents (Seton Hall University, 2014). UV lamps are currently popular in the field of water disinfection, which is the focus of this research effort. These lamps are effective in directly deactivating bacteria and other pathogens by interfering cellular functions through disrupting the deoxyribonucleic acid (DNA) chain within bacteria or spores (Wuertele et al, 2011). Recently, interest has also grown in the use of ultraviolet light to aid the production of hydroxyl radicals from peroxide in water. These highly reactive radicals can be used to oxidize organic pollutants (US Peroxide, 2012). Due to some of the issues experienced with conventional florescent lamps, LEDs are of interest in this field of study.

LEDs are of particular interest for this research for various reasons, including their durability during handling and transit (especially important for deployed settings), their ability to be altered to multiple different wavelengths for different purposes, and the fact that they do not have to be disposed of as hazardous waste, unlike florescent lamps which contain mercury. Further, these devices can be cycled rapidly (i. e., they can turn on and off quickly), are light weight and compact, have a narrow bandwidth, and require much lower voltage input than the typical mercury lamps. Additionally, these devices have a potential for higher efficiency and longer life.

The focus for this research included improving an understanding of the life, power consumption, and efficiency of the UV LEDs. A study conducted by Gadelmoula et al (2009) explored the inactivation of Escherichia coli using continuous UV output and a pulsed 9.1 percent duty cycle output using the same peak power. This research indicated that the time integrated current required to drive the UV LED was more than ten times the energy as the pulsed current to produce the same result. These results suggest a pulsed system could be designed to perform the same task as a continuous system while extending the life and reducing the power requirement of the UV LEDs. However, as this researcher did not quantify the power output of the UV LEDs in pulsed and continuous modes, it is not clear that the pulsed configuration exposed the bacteria to optical power that was only 9.1% of the continuous condition. Therefore, the goal of the present research was to enable the characterization of UV LEDs in air and water when the UV LEDs are driven continuously or in a pulsed mode to permit the power from the UV LEDs and the dose to be quantified.

Problem Statement

There are three related projects that will be referenced throughout this thesis. The hydroxyl radical project refers to using UV LEDs and hydrogen peroxide to produce hydroxyl radicals and use the radicals to break down hazardous chemicals. The second project that will be referenced is the drinking water disinfection, which refers to using UV LEDs to interrupt the DNA chain in bacteria. The third project that will be referenced is the model that will take all of the data collected to predict how to optimize the UV LEDs. There needs to be a way to quantify the hydroxyl radical production and DNA destruction as a function of a known optical power reference. Currently, there is no standard measurement method for assessing optical power of an immersed UV LED. Further, characterization of UV LED power output in air or water has not been fully addressed.

Research Objectives/Questions/Hypotheses

The objective of this research effort is to explore the differences in how UV LED optical performance changes in water as compared to air. The two parameters that are expected to be different, which are most important to the performance of the UV LED, are the temperature of the UV LED and the efficiency of light emission into the medium of interest, which in this case is water. The hypothesis is that water will decrease the temperature of the UV LED, which typically extends UV LED lifetime and improves output efficiency (Lenk/Lenk, 2010). Further emitting energy directly into water, which has a higher index of refraction than air, will increase the power efficiency of UV LEDs by improving the coupling of energy into water. The data collected from this research will then be used by a companion researcher to create a model that will be able to predict power consumption, lifetime, and AOP utility for the UV LEDs being studied. This model will also have the ability to estimate the parameters for the UV LEDs that are being driven in pulsed or continuous current modes. This model will then be used to optimize the UV LED for use in water treatment. Another innovative feature of this project includes applying current of various durations to the UV LEDs rather than continuous current, which is expected to reduce the power requirements and extend the life of the UV LED when applied in water treatment.

The specific questions this project is expected to be able to answer are:

1. What is the relationship between UV energy output and input current for commercially-available GaN UV LEDs when these lamps are driven continuously or pulsed at various duty cycles?
2. Is there a change in the relationship between UV energy output and input current when these GaN UV LEDs are immersed in water than when measured in air and can this relationship be explained by a simple Snell's Law relationship?
3. How do we measure power efficiency of UV LEDs in water?

Assumptions/Limitations

There were several limitations that affected this research. The project was restricted to using commercially available, off-the-shelf UV LEDs at 240, 260, 265, and 270 nm wavelengths (SETi, 2014). Sensor Electronic Technology, Incorporated (SETi) was one of the few manufacturers of these UV LEDs worldwide and therefore the they would be sourced from this supplier. Another important limitation was the variability of the vendor's UV LED devices. This constraint was also due to the cutting edge nature of this technology. This issue is expected to be eliminated or at least reduced significantly as the technology becomes more advanced. The need to understand the reflectance of Spectralon®, a coating material inside of the integrating sphere used in this study, introduced another constraint. This material had not been well characterized in the ultraviolet range and had not been well characterized when interfacing with water rather than air. Reflectance measurements were conducted using the CARY 5000 (CARY 5000, 2011), a ultraviolet and visible spectrum photospectrometer, in the AFIT Physics Department, which was not designed to permit water measurements. One final limitation was the integrating sphere, which is used to measure luminous flux and optical power, was not received until late in the project. This limitation forced the development of measurement techniques in a shorter than desired time period. Further, as the manufacturer of this instrument had no previous experience in constructing measurement devices for measuring optical power output in water, this arrangement was speculative.

An assumption made in this work is that the results obtained using the current families of UV LEDs can be extrapolated to other UV LEDs. Further, UV LED measurements are assumed to be representative of UV LED performance in the water reactors used in companion portions of this research.

II. Literature Review

A study relating optical power and the associated log kills of the bacteria being studied was conducted in one of the articles reviewed. This study proposed various equations accounting for losses experienced during data collection (Gadelmoula et al, 2009). Whenever calculations have to be performed, a certain amount of error is introduced. The more precise way to conduct the experiment would be to eliminate surfaces that have to be accounted for as losses. In some instances, there may not be a way to reduce the effect of losses. However, in Gadelmoula et al's (2009) study there are a few losses that could be eliminated from the experiment. For example, this research imposed an air gap and a quartz cover between the UV LED and the water being disinfected which resulted in optical losses, whcih had to be estimated. Snell's law describes how light bends went it transmits through different media. The media of most interest for this research is air and water. Since the index of refraction is greater for water than air, there is a high likelihood that water will be a more efficient media for light to travel through than air. However, a more efficient way to irradiate a chamber where disinfection (and chemical oxidation) is the objective is to have the UV LED submerged in the media of interest (Gadelmoula et al, 2009).

A 9.1 percent duty cycle was studied for the air stream disinfection was 9.1 percent using a pulse that was oscillated between 10 ms on and 100 ms off (Gadelmoula et al, 2009). The desired current for water disinfection, which was an important part of this research effort, was 20 mA (Wuertele, 2011). The better the efficiency and the longer the life of the UV LED, the more efficient the water disinfection will be. The use of a pulsed light source with reduced average power was expected to extend the lifetime of the UV LED for a given power efficiency. The use of this pulsed signal provided an initial set of conditions to determine if similar results could be obtained when decontaminating water. Since drinking water is an ingestion hazard for humans, this may prove to be a

very useful technology for commercial applications and the Department of Defense for state-side compliance and during wartime campaigns when the purchase of water or large scale disinfection may not be an option.

For the scope of this project, an integrating sphere is the primary instrument used to obtain optical power measurements. These devices are particularly useful when measuring the output from devices with output that varies as a function of angle as they permit the energy across all angles to be integrated. Integrating spheres are often used to measure luminous flux, but are also useful in measuring optical power. The preferred size of the sphere is four to five times larger than the diameter of the light source (Lenk and Lenk, 2010). These spheres may range in size from a few centimeters to large enough to enclose a human. In an integrating sphere, light is scattered from the source in all directions and reflected from the highly reflective material which coats the inside the sphere, until the light encounters a collector. This collector then permits the luminous flux (optical power) to be integrated across all angles. The illumination source is typically placed inside the sphere. Spheres are usually designed so the collector is behind a baffle, which blocks the light to increase the accuracy of the instrument. This baffle is especially important because it prevents the detector from receiving light directly from the illumination source, which can adversely affect the measurement. The integrating sphere must be calibrated to a standard light source, which is traceable to a national or international standard. A light source must be used as a calibration source to account for the inner surface of the integrating sphere, since it is not 100 percent reflective. The preferred collector is a spectroradiometer, which separates light by wavelength and measures the amount of light at each wavelength. A photometer can be used to measure luminance of a visible light, but is only capable of measuring lumens (not spectral information) (Lenk and Lenk, 2010).

For an integrating sphere to operate properly, it is important to have a highly reflective surface inside the sphere. Further, this surface needs to scatter well so that all angles of light emitted from the light source can be mixed. This is necessary to permit measurements to be captured from the exit or measurement port, which is a very small area. The inner surface of most modern laboratory spheres are coated with material called Spectralon®, which is a branded version of a Teflon® material used by Labsphere®\. Spectralon® has a few interesting characteristics that are important to note. First, Spectralon® has a high reflectance across the entire visible spectrum and far into the infrared. Labsphere®\claims reflectance for Spectralon® from wavelengths 250 nm to 2500 nm to be as high as 99 percent (Labsphere, 2014). However, it has been reported that the reflectance of Spectralon® is greatly reduced for short wavelengths (Moller, 2003). In fact, Spectralon® has a reflectance of approximately 90 percent for wavelengths between 254 nm and 365 nm (Moller, 2003). Further, a 30 percent reflectance was observed at a 300 nanometer wavelength in a study cited by Moller (2003).

Another important point to note for future research is the degradation of Spectralon®. For wavelengths less than 450 nanometers, simply exposing Spectralon® to normal room light can cause degradation. Degradation appeared to occur after the first irradiation at these wavelengths, even if no further irradiation occurred. The largest degradations were observed for samples that were observed for more than one year (Moller, 2003). Another article suggested that polycyclic aromatic hydrocarbons in the ambient air could be a possible catalyst for this degradation (Ping, 2003). When the fluorescence spectra waere analyzed for multiple integrating spheres. Florescence of Spectralon® decreased between 250nm and 400 nm as the wavelength of the laser increased. The decrease in florescence is not intrinsic to the polytetrafluoroethylene PTFE (Teflon) material inside of the spheres. The variations are suspected to be associated with contamination of the PTFE inside of the

spheres with volatile impurities from the manufacturing process or exposure to a contaminated environment (Ping, 2003). This research demonstrates that PTFE should have a relatively high reflectance for UV energy with wavelengths longer than 250 nm, albeit slightly lower than that for visible energy. The previous research did not discuss the effect that water has on the reflectance of the PTFE. Further, that PTFE permits a high degree of diffusion because it is porous, which allows light to enter the surface and reflect many times within the material. This suggests that water could have some effect on the diffusive properties of this material and thus the way light interacts with it.

For this research, it is important to understand the function of LEDs. As the name infers, LEDs are diodes and as such permit current to flow in only one direction. LEDs are broken into two main classes: small devices and power devices. Small devices are sold by the tens of billions every year and usually range in power from 20 mA to 100 mA. Small devices are seen in all kinds of applications, but a few examples would be automobiles, cell phones, and traffic lights (Lenk and Lenk, 2010). Large devices are relatively new, as these devices have come into existence within the last 15 years (Kuo et al, 1990). These devices produce enough light to serve as a true illumination device and can draw 0.1 to 1.0 mA (Cree, 2014). UV LEDs have only recently become available and therefore have very few manufacturers. Sensor Electronic Technology, Inc (SETi) is a small company, which developed UV LED technology using funding primarily from Defense Advanced Research Projects Agency (DARPA) for use in sensing applications. As such, SETi is one of only a few vendors that offer these UV LEDs (SETi, 2014). Ohm's law does not apply for diodes. The relationship between voltage and current is not linear, but is rather exponential. Therefore, LEDs are considered current devices, as the energy output of the diode is linearly correlated with the current that is passed through the device. Theoretically, the current flowing through the LED would be dependent upon the voltage to which the diode is exposed. In reality this relationship is more complicated as other factors, such as the

temperature and the size of the device, also play a role. This is a key point because overdriving an LED may cause an increase in power output, but overdriving may also cause an increase in temperature, reducing efficiency and power output causing a shortened life of the LED. Efficiency is defined as the ratio of the power output to the power input, measured in watts. Efficiency is generally reduced as the LED warms up. Another important performance parameter is whether the LED is being pulsed or is being used as continuous wave. If the LED is pulsed at a high frequency, the device is dependent on the average power for the temperature. If the LED is pulsed at a low frequency (slow), there may be adequate time for the die in the LED to cool, which can substantially affect the life of the LED. The thermal time constant of the LED then determines the speed of degradation (Lenk and Lenk, 2010).

Typically, current increases with an increase in input voltage, once the voltage exceeds a threshold voltage. Overdriving, which is sending too much current through the LED, can significantly improve the output of the LED, but typically drastically reduces the lifetime of the LED (Lenk and Lenk, 2010)

For a direct current power system, the input power is calculated by multiplying the current and the voltage. This is not a trivial calculation, however, since the measurement of the current and voltage must be taken at the same place. Therefore, the use of a digital voltmeter will likely be necessary to determine the efficiency of the device, as well as measurement of the energy output of the LED at the known input power (Lenk and Lenk, 2010).

The final point that will be discussed in this chapter is what current data exists on optical power measurements. Currently, no optical power measurements exist for UV LEDs in water. This research intends to characterize the optical power for 240 nm, 260 nm, 265 nm, and 270 nm UV LEDs. These UV LEDs are of particular interest due to their applications in water treatment.

Understanding the optical power is important for many reasons. This research effort focuses on using these measurements to understand the voltage needed to maximize the UV LEDs performance for the disinfection of drinking water and the production of hydroxyl radicals.

III. Materials and Methods

This chapter will discuss the experimental apparatus, the methods used to collect the data, and the experimental design for this research effort that will be applied within this document. Three experiments were conducted with several instruments required for each. To understand optical performance of the integrating sphere, a characterization of the reflectance of Spectralon® was first conducted. For the reflectance measurements, a CARY 5000 was used (CARY 5000, 2011). This instrument was not intended to operate with water, so a sample holder was fabricated to enable these measurements. A computer program (DASYLAB) (DASYLAB, 2014), a data acquisition device USB driver (Measurement Computing, 2014), and a driver board were required were required to drive the UV LED for the air and water experiments. The air and water experiments had their own required hardware and software programs. A primary focus of this research was to quantify and compare the optical performance of UV LEDs in both air and water. This will allow the extension of LED use from air, where they are typically characterized, to water, which represents the environment under which the UV LEDs will be applied for water purification.

Apparatus

Reflection Instrumentation

The apparatus used to support these measurements was the CARY 5000, photospectrometer, from the Air Force Institute of Technology's Physics Department (CARY 5000, 2014). The CARY 5000 was designed to perform measurements only for a sample in air. To permit measurements to be taken in the water matrix with the CARY 5000, an apparatus had to be created to hold the Spectralon® sample. This sample holder was designed to fit in the CARY swivel table sample holder. In addition to this holder an insert was designed to hold a Spectralon® sample, which was a circular sample having about a 1 inch diameter. Figure 1 shows a picture of the sample holder and

insert. The sample holder was a water tight box made predominantly of a plastic material with a quartz window. The quartz window allows for effective light transmission in order to measure the reflectance of the Spectralon® in the insert.

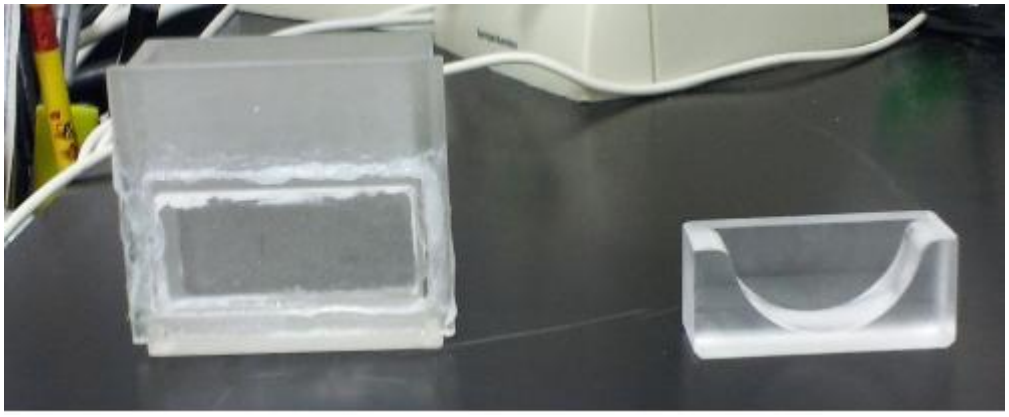

Figure 1: Sample holder for the CARY

Figure 2: CARY 5000

The CARY 5000 measured reflectance as a function of angle and wavelength. The primary purpose of this device was to measure transmission or absorbance of a clear or translucent solid.

The reflectance measurement was an additional capability of the CARY. Reflection may be broken into two categories: specular and diffuse (CARY 5000, 2011).

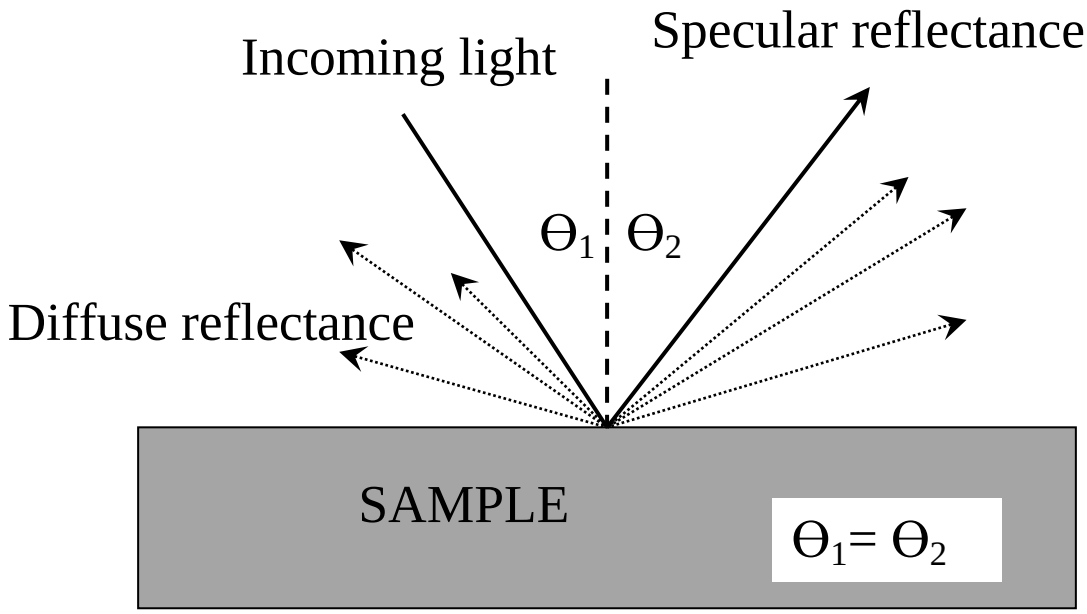

Figure 3: Specular versus diffuse reflectance

Specular reflectance refers to a mirror-like reflection off of a sample surface. Diffuse reflection refers to the surface of the sample scattering light in all directions and angles. The data that the CARY's software produced was based on background measurements, derived from a 100 percent reflection, a zero percent reflection, and a reflectance measurement of the sample in the sample holder. These measurements were collected using a series of mirrors, a light source, a sample holder, and a data collection port. For further details of how the beam path operates in the CARY and for a better understanding of the geometry inside of the CARY, reference page five of the instrument manual (CARY 5000, 2011).

Optical Power Measurements in Air

Several instruments were applied to permit characterization of the UV LEDs. The following are the instruments applied to enable the measurements of the UV LEDs in air.

DASYLAB

A drive signal for the UV LEDs was produced using the DASYLAB program on a computer inside DASYLAB (DASYLAB, 2014). Two different DASYLAB programs were designed and applied, one for the continuous steady state signal and another to produce a pulsed signal. The program for the continuous wave signal was intended to input a desired voltage, record and plot the output voltage, and calculate the current. The pulsed program permitted the user to define a square wave having a given duty cycle and frequency. While the DASYLAB software provided the flexibility necessary for this research only a single output could be generated with a pulsed signal and this pulse signal was limited to only about 20 Hz. For this research, a signal having a constant voltage was generated for the continuous drive signal while a signal having a frequency of 9.1 Hz and a duty cycle of 10 percent was created to generate the pulsed signal.

Data Acquisition Device (DAQ)

The Measurement Computing USB 2408-2AO DAQ received a command signal from the USB port on a computer as created in the DASYLAB software (DASYLAB, 2014). The box was of outputting a signal, which was limited to 10 volts. To validate the DASYLAB program was sending the proper wave signal to the driver board for the pulsing of the UV LED, an oscilloscope was used.

Oscilloscope

The WON PDS50221 oscilloscope was used to validate the frequency, duty cycle, and voltage of the pulsed signal provided by the DAQ (Measurement Computing, 2014). This same device was

also used to validate the appropriate signal was being provided by the driver board to the UV LED. The Oscilloscope was also used to measure the voltage drop across a 50 ohm resistor to determine the appropriate current was being provided to the UV LED in the pulsed mode.

Digital Multimeter

To ensure the DASYLAB program was sending the proper voltage to the driver board, a Extech Instruments Non-Contact Voltage Detector (S/N 12052602) multi-meter was used to measure the voltage coming out of the DAQ and at the fixed resistor where the UV LED was being driven (Extech Instruments, 2014). In addition, the voltage drop across the resistor was also measured with a multi-meter to be able to calculate the current being sent through the UV LED.

Driver Board

The electronics driver board contained a power supply and various electronic components that drove the UV LED. The power supply was a simple transformer based +/- 24 volt system capable of 0.6 amps. 24 volts provided the flexibility to provide larger than necessary voltages and 0.6 amps is adequate for steady state operation of several UV LEDs since each UV LED only uses 20 mA. The heart of the driver board was an opamp, which operated off of the DAQ output voltage. The opamp created an isolated circuit with the power supply, allowing large amounts of amperage to pass without sending amperage back to the DAQ. This eliminated power feedback loop voltage and amperage, while the driver board supplied the amperage to the UV LED.

The DAQ was attached to the common ground for all measurements and output. The output voltage attached to either the a or b input voltage pin hole. The op amp opened the isolated circuit to the voltage set by the input. Amperage then flowed from the power supply to the opamp to the UV LED. Each branch had a resistor and pin holes for electrical measurement in series with individual UV LEDs, although this research effort only required one UV LED to be used in each experiment. The

resistors were initially selected to provide protection to the UV LED by only allowing 20 mA at maximum input voltage (10 volts).

Spectral Radiometer

This Labsphere spectral radiometer instrument was used to measure the amount of energy integrated across wavelengths ranging from 210 nm to 400 nm.

Deuterium Lamp

The D2 Deuterium lamp (S/N 667329) was used as a calibration source, which is intended to provide a background subtract for the less than 100 percent reflectance of the integrating sphere (Ocean Optics, 2014).

Chiller

The Arroyo Instruments chiller was intended to control the temperature inside of the integrating sphere. The chiller was controlled by the Illumia Pro software (Arroyo Instruments, 2014).

Shutter

The Labsphere shutter was the device that allowed the light scattering in the sphere to be analyzed or blocked from entering a fiber optic cable which is attached to the spectral radiometer (Labsphere, 2014). This shutter was included in the design since the fiber optic cable can degrade from UV exposure. The shutter ensured that this exposure only occurred during the active measurement time.

Labsphere Control System

This tower contained the spectral radiometer, the digital readout for the chiller, the power light for the calibration lamp, and the power switches for all of the instruments. This entire system was driven by the Illumia Pro software installed on the laptop computer (Labsphere, 2014).

Illumia Pro Software

This software was used to analyze the amount of output power the UV LED provided over the wavelengths 210 nm to 400 nm. This allowed the user to see where the largest amount of power output existed, which should have been focused mostly at the wavelength the UV LED was designed to.

Optical Power Measurements in Water

For measurement of UV LED performance in water, the apparatus was modified to be able to place the integrating sphere into water. The modifications include:

Fish Tank

A 50 gallon fish tank served as the area to submerge the integrating sphere into water. The sphere had legs placed on the bottom of it using two fabricated stainless steel pieces and a bolt fastened to the bottom port of the sphere.

D2000 Deuterium Lamp (S/N 0052500730)

The calibration lamp worked the same for this experiment in air except that the unit was not built into the control system.

Extended UV LED leads

The leads for the UV LED had to be extended using additional wire. These wires were soldered together and laced with silicone to prevent water intrusion into the electrical wires that power the UV LED.

Figure 4: Electronics box for the integrating sphere

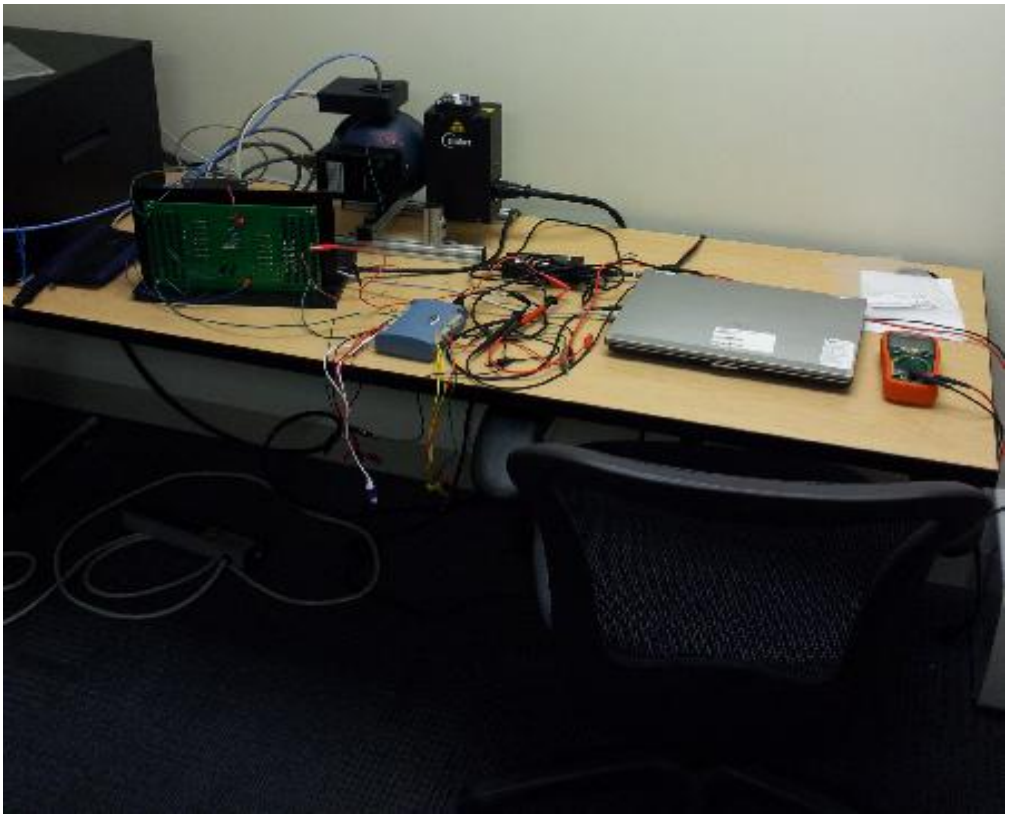

Figure 5: Air measurement setup

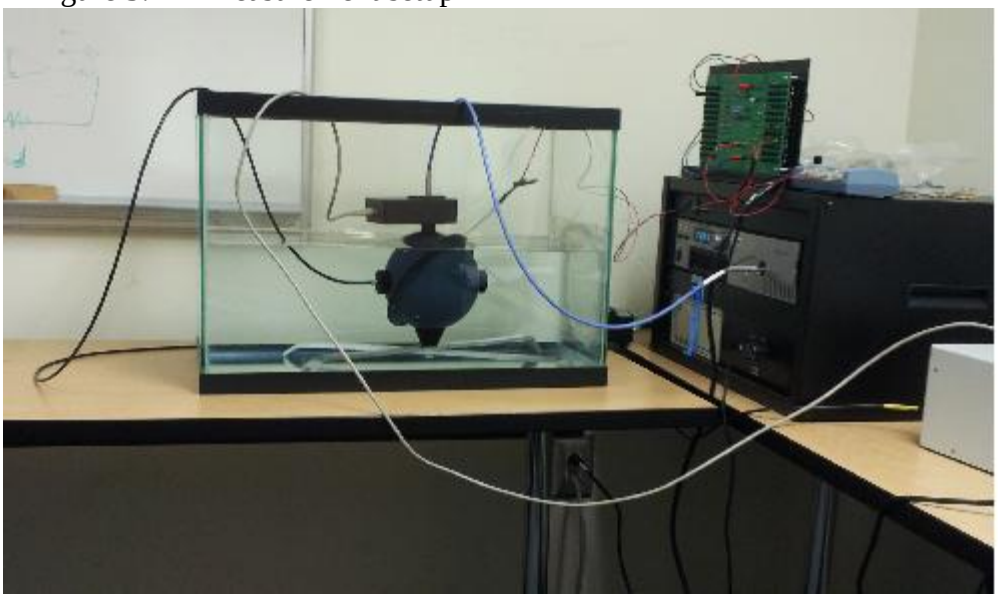

Figure 6: Water experiment setup (1/2)

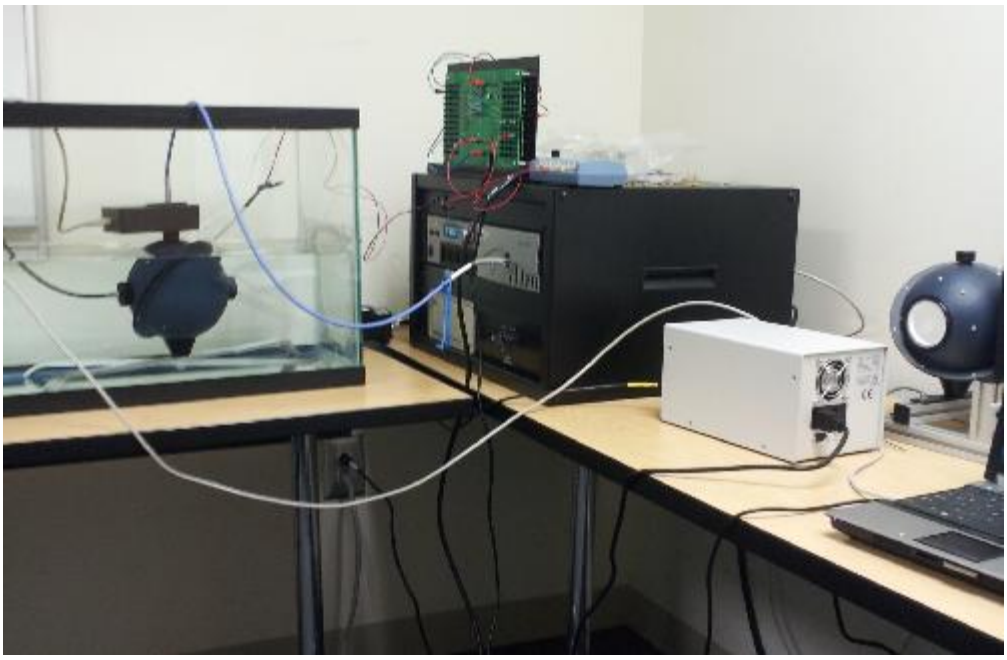

Figure 7: Water experiment setup (2/2)

Figure 8: Driver board and DAQ

Method

Reflectance Measurements

The first set of experiments determined the reflectance of materials to be used within the measurement apparatus and within the water reactors. These reflectance measurements are designed to permit the determination of the reflectance of the materials of interest as a function of wavelength and angle. The materials that were to be measured by the CARY included materials that were being considered as candidates for the internal surface of the measurement sphere or the water reactor. These measurements should permit characterization of the reflectance in air and in water.

A scan of the reflectivity was performed from 200 nm to 400 nm and was analyzed from a 20 degree reflection to a 70 degree reflection. Since the sphere was intended to send the signal for the optical power out of a small port in the side of the sphere, coating the inside of the sphere with something that was very reflective, which minimized the amount of loss into the sphere. These losses were expected to be quantified in the calibration and will be corrected for in further measurements. The CARY also has a background correction feature for the measurements with respect to the reflectiveness of the Spectralon® sample. The CARY first prompted the user for a sample to represent 100 percent reflectivity, typically a mirror, and then asked for a sample to represent zero percent reflectivity, typically a dense cardboard material.

Optical Power Measurements in Air and Water

DASYLAB 12.0 was the software chosen to control the driving of the voltage and the pulsing of the UV LEDs. Details of how the DASYLAB programs that were used may be found in the Appendix. This software sent a signal to the DAQ. The signal was then sent from the DAQ to the driver board. The driver board consisted of a power supply and seven 56 ohm fixed resistors. The UV LED chamber had the leads for the UV LED, which connect to the drive board so the UV LED could obtain the necessary voltage to turn on. Illumia Pro was the software the integrating sphere used to process the output power of the UV LED. This software was linked to the shutter, which was linked to

the spectral radiometer, and the main box that had the chiller digital readout, the power switch for the spectral radiometer and the deuterium lamp. The shutter was mounted to the top of the sphere and had a fiber optic cable that connected it to the spectrometer. An Ocean Optics D2 deuterium lamp was mounted to the side of the sphere. The chiller was intended to control the temperature in the UV LED chamber to the desired temperature. This is a key point since temperature is one of the main factors that affects UV LED performance.

The next step in conducting this research was to set up the air measurement experiment. Figure 9 is a block diagram that outlines the process for the collection of experimental data. The first line shows how the UV LED obtains power to turn on. The computer loaded with the DASYLAB software to drive the DAQ, which in turn drove the driver board. The driver board then provided the necessary voltage to the UV LED chamber to illuminate the LED. The second line shows how the software interacted to collect the necessary data. DASYLAB allowed the user to enter an input voltage and a pulse signal, if necessary. That signal was then transferred to the UV LED inside of the integrating sphere, which transmitted through the shutter to the spectral radiometer to provide the information to plot the integrated power over the 210 to 400 nm spectrum in the Illumia Pro software. Prior to powering the UV LED, a calibration with a known source was performed to correct for the interference from the coating on the inside of the sphere. Once this background correction was performed, the UV LED was powered and the continuous and pulsed experiments begun. The third line shows the procedure for performing the calibration. The Illumia Pro software prompted the user to warm up the lamp for a few minutes. Once the lamp was warm, the data for how the light scattered in the sphere began to process. This process lasted several minutes depending on the ratio of light to dark inside of the sphere. The fourth line shows the process of running the experiments. Once the

calibration was performed, the UV LED was powered using the process outlined above. DASYLAB was then used to run the continuous and pulsed configurations.

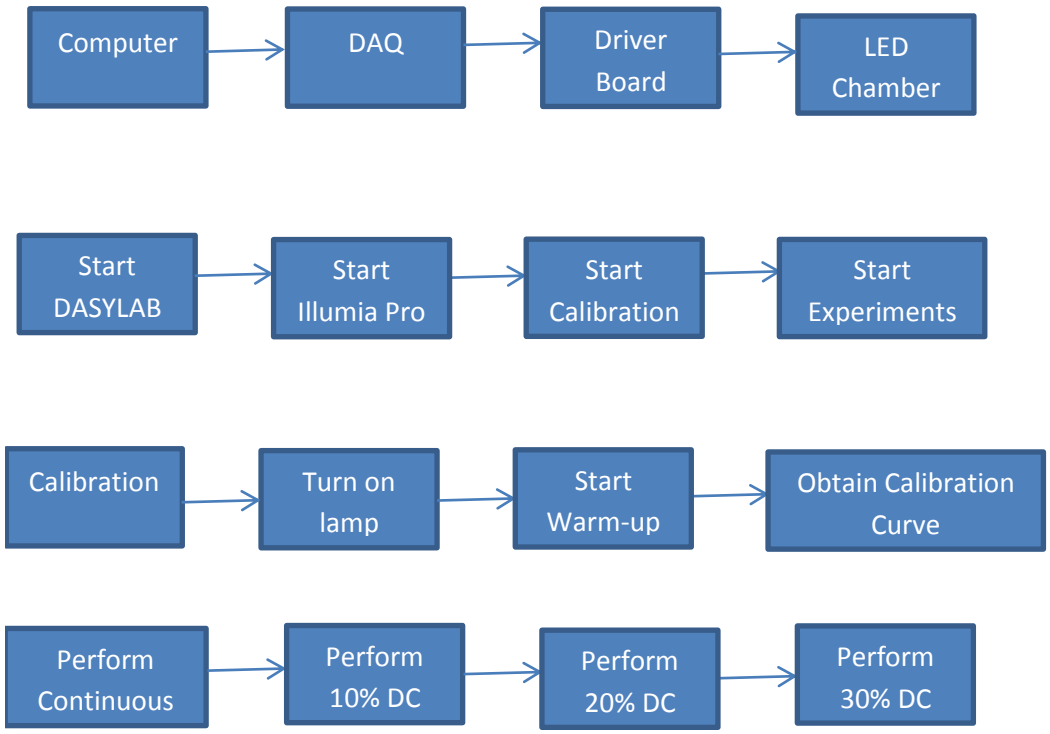

Figure 9: Block diagram for experimental setup

Experimental Design for UV LED Characterization

Reflectance Measurements

A less traditional approach was used for this research effort. An ultraviolet polished aluminum mirror inside the insert with two metal spacers were used for the 100 percent reflectance background subtract. Spacers were used to assist with holding the mirror in a vertical position to minimize the angular reflection differences for holding the mirror at an angle. The sample holder with the empty insert inside of it was used for the zero percent reflectance. Once this background was collected, the actual reflectance measurements were accomplished. The Spectralon® was first measured inside of the sample holder in air. Then, a separate background was collected with the sample holder filled with de-

ionized water. Once this background was measured, the Spectralon® was submerged into the water filled sample holder and analyzed by the CARY.

Optical Power Measurements in Air

For the sphere measurements, there were two different parts for each air and water experiment. These two parts included continuous wave measurements and pulsed wave measurements. For the pulsed wave measurements, a frequency of 9.1 Hz and a duty cycle of ten percent was chosen to because of referenced published data for the 10 ms on and 100 ms off, which was approximately a 9 percent duty cycle. That study did not reference the output power, but it did relate to other experimental data. To further characterize the pulsed output power, a duty cycle of twenty percent and thirty percent were also used for each UV LED.

For all continuous wave measurements, the peak wavelength, temperature, current, input voltage, total power, and selected power were recorded. The selected power was the amount of power between the wavelength bands chosen by the user in the Illumia Pro software. For this project, the center between the lines was the wavelength for the UV LED being characterized. The current of most interest, since there was referenced published data for a different project for this current, was 20 mA. However, to obtain a better understanding of what the output power looks like as current is increased or decreased, several measurements were taken below and above 20 mA. The output power and the current were then plotted for comparison. It was expected that this would be a linear curve. Another plot was also created to predict the pulsed wave current, since that could not be measured directly. This plot used an exponential curve using the voltage and current from the continuous measurements.

For the pulsed wave measurements, the input voltage, total power, selected power, and temperature were recorded. The output power was compared to the current in a plot. In addition, an overlay plot was created by comparing a ten percent duty cycle, a twenty percent duty cycle, and a

thirty percent duty cycle. To better understand if there was a linear correlation between the different duty cycles, a two times and three times the ten percent duty cycle lines were created.

The design for what data needed to be captured was the same for both the air and water measurements. Figures 10 and 11 outline what measurements were intended to be taken when beginning the project. However, since the chiller did not work properly due to a shorting issue, the fixed compared with the not fixed temperature comparison could not be made.

		Temperature		
		Fixed		Not fixed
		25°C		
Used	Serial #	Temp (°C)		Temp (°C)
LED 1				
LED 2				
LED 3				
New				
LED 1				
LED 2				
LED 3				

Figure 10: Design Matrix for temperature readings

Continuous					Current					
Constant Current					Pulsed					
	Serial #	Power			Power			Duty Cycle		
Used		10 mA	18 mA	20 mA	10 mA	18 mA	20 mA	10%	20%	30%
LED 1										
LED 2										
LED 3										
New										
LED 1										
LED 2										
LED 3										

Figure 11. Design Matrix for optical power readings

Optical Power Measurements in Water

The final step for collecting the necessary data for this research project was to obtain the water measurements. The water measurements consisted of the second DASYLAB program sending the pulse and voltage signals through the DAQ to the driver board to the integrating sphere, which is sbumerged into a 55 gallon fish tank filled with distilled water (reverse osmosis water). To fasten the UV LED chamber inside of the integrating sphere, a plate with three holes was used to mount to the side of the sphere. Two screws with taps mounted the UV LED chamber to this plate and the UV LED leads were routed out the other hole in the plate. One of the difficulties with this experiment setup was that the shutter is not water safe. The shutter is necessary for collecting the spectrometer data to view in the Illumia Pro software. To ensure water intrusion did not occur a blue self-forming gasket was used to seal the UV LED prongs and the UV LED leads were protected by soldering the wires together and using silicone. A Deuterium 2000 calibration lamp was used for calibration. This lamp was an external unit that was connected to the side of the sphere with a fiber optic cable. The integration time for this was 900,000 ms and averaging of one. This averaging is referring to the amount of times the Illumia Pro software scans the sphere to increase the accuracy. Since the noise was relatively high, a scan of one was necessary due to the amount of time that one scan took.

In order to obtain a reasonable signal to noise ratio, the integration time was set to 150 ms for continuous wave measurements and 440 ms to 990 ms for pulsed wave measurements. Calibration was performed every time the Illumia Pro software was started for the first time that day (calibration at 150 ms and averages of 20 taking about 6 minutes). While published data states that UC LEDs can be instantly turned on, for consistent measurements a one minute warm up period was included. This was established based on the difference in output power with and without a warm-up period. There was

approximately a five percent increase in power output after the one minute warm up in both cases it was tested.

IV. Results

The measurements described in Chapter III are quantified in this chapter. While there were numerous measurements taken for the different experiments, only the plotted results will be shown in this chapter. Values that were used to create the plots may be found in the appendix. The results are divided into three sections with the first section detailing the reflectance of Spectralon® in air versus water. The following two sections describe the performance of the UV LEDs in air and then compares these results to initial results for UV LEDs in water.

Reflectance Measurements

The reflectance measurements and the sphere measurements were obtained using the CARY 5000 and Illumia Pro respectively as described in Chapter III. The reflectance measurements were intended to understand how the reflectance of Spectralon® changes in water verses air. As noted earlier, Spectralon® is typically selected as a coating for spheres because of two unique properties. First, it provides extremely diffuse reflection, permitting it to disperse the energy such that any light ray produced by the source is equally likely to impinge upon the sensor. Second, it has a high reflectance across the entire visual range, where these types of measurements are being taken.

The reflectance measurements then permitted both the quantification of the uniformity of reflection across a range of angles, permitting an assessment of the diffusion of the energy and across a range of UV wavelengths, permitting the assessment of the reflectance of the material as a function of wavelength.

Figures 11 through 16 provide results for the reflectiveness of Spectralon® in water versus air for multiple angles ranging from 20 to 70 degrees. Reflection, by definition, cannot be negative, however, negative values appear in the plots. The most logical reason for these negative values to be present in the plots is the interference of the sample holder. The reflection measurements reading

negative are assumed to be attributed to the correction which was applied to remove the effect of the window on the sample holder. Therefore, the absolute magnitudes of the measured values are questionable because the CARY 5000 was not designed to accommodate a sample holder. Future research will likely be needed to truly understand the absolute reflectance of Spectralon® to UV energy in water.

With the presence of negative values as a caveat, the relative trends in these plots are still of interest. These figures indicate the reflectance of Spectralon® was higher in water for 20 to 40 degree angles, but lower for 50 to 70 degree angles. Therefore, it would appear that the Spectralon® is not as Lambertian in water as in air, because the reflectance in water is higher for small angles (angles near the specular reflection angle) and smaller for large angles. However, the sample of Spectralon® that was analyzed was very diffuse since it had a reflectivity of less than one percent for any given angle while having a high overall reflectivity.

While the slope of the curves might be steeper in one plot than the other, the reflectance decreases in an exponential decay shape as wavelength decreases for all plots. For 20 to 40 degrees, there seemed to be a threshold around 250 nm for the water sample where the reflectance begins to reduce, while the threshold for the air sample occurred around 300 nm. For 50 to 70 degrees, the reduction occurred around 300 to 350 nm. The wavelength range of interest for this research is from approximately 230 nm to 280 nm since the UV LEDs being studied are 240 nm, 260 nm, 265 nm, and 270 nm. Focusing on the characteristics of Spectralon® at 250 nm, which was very close to the wavelengths of interest, a few key points may be made. Spectralon® in water appears to have a higher reflectance from 20 degrees to 40 degrees. Spectralon® in air is much lower for this degree of rotation. At 50 degrees, both in air and in water Spectralon® is well above zero percent reflectance. For 60 to 70

degrees, Spectralon® in air continues to be well above zero percent reflectance, while in water it appeared to stay very close to zero percent reflectance.

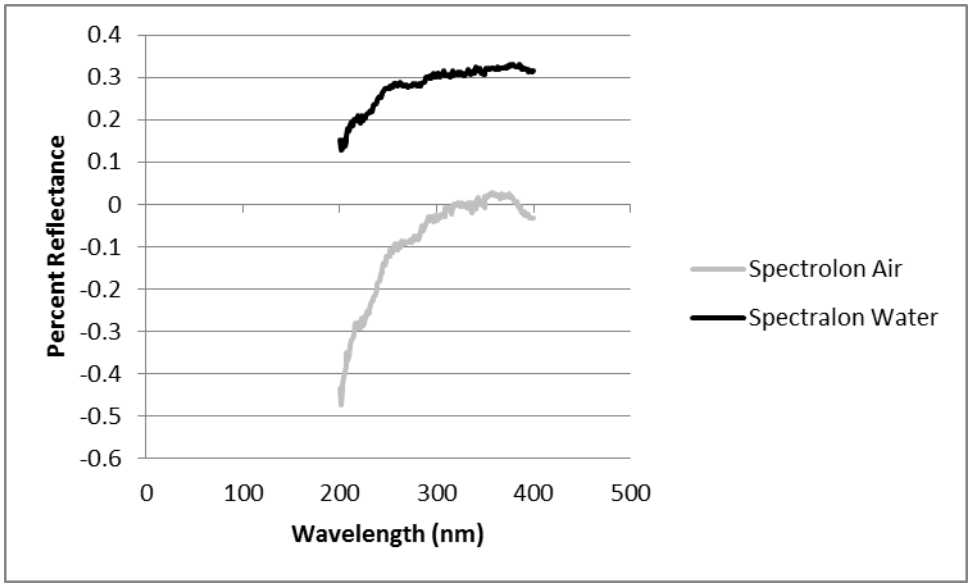

Figure 12: Spectralon® reflectance at 20 degrees

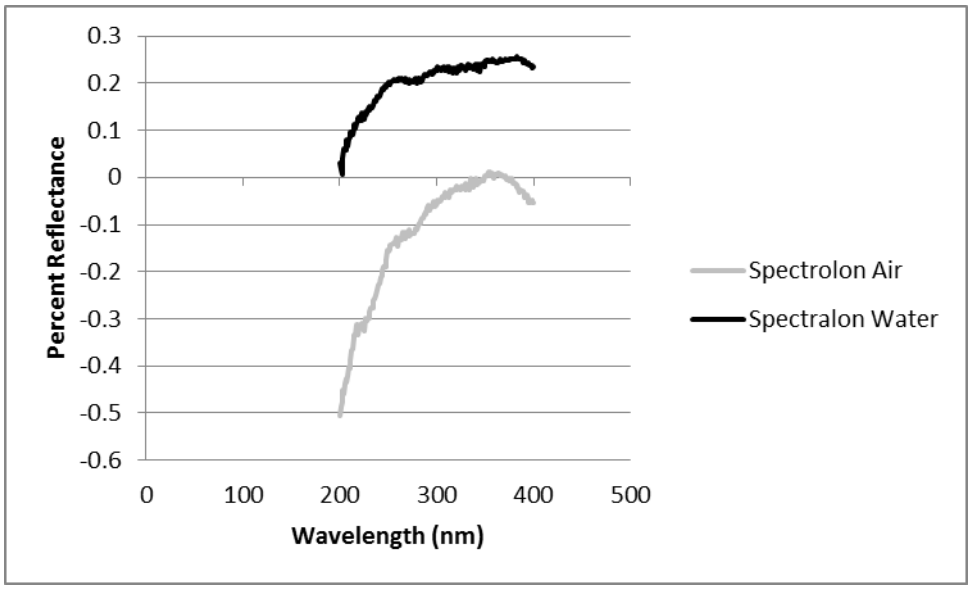

Figure 13: Spectralon® reflectance at 30 degrees

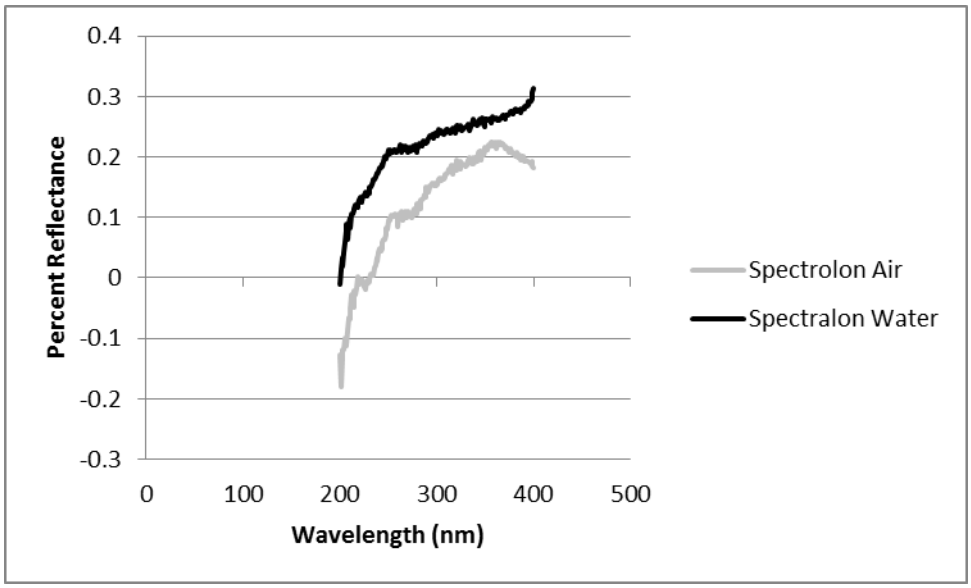

Figure 14: Spectralon® reflectance at 40 degrees

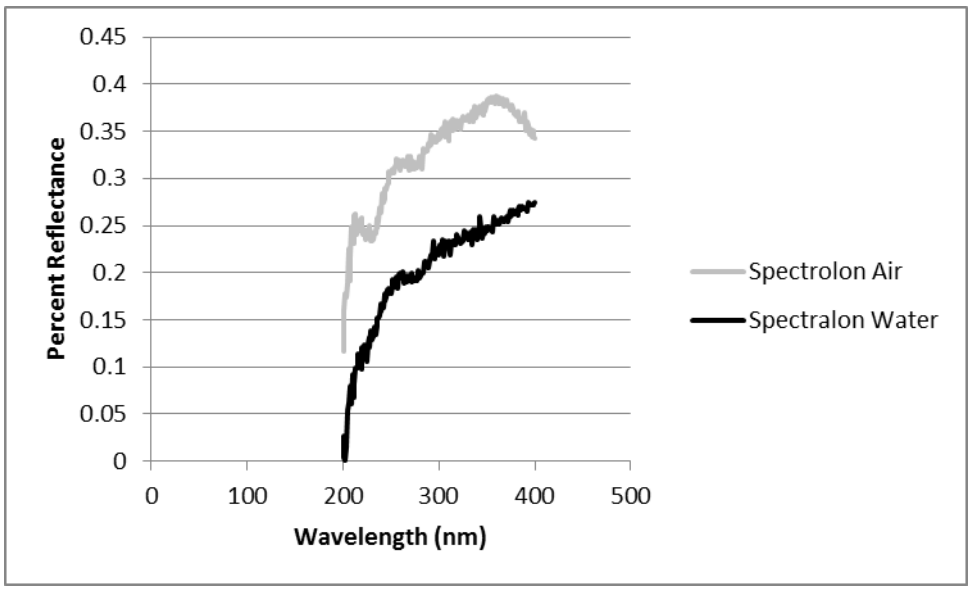

Figure 15: Spectralon® reflectance at 50 degrees

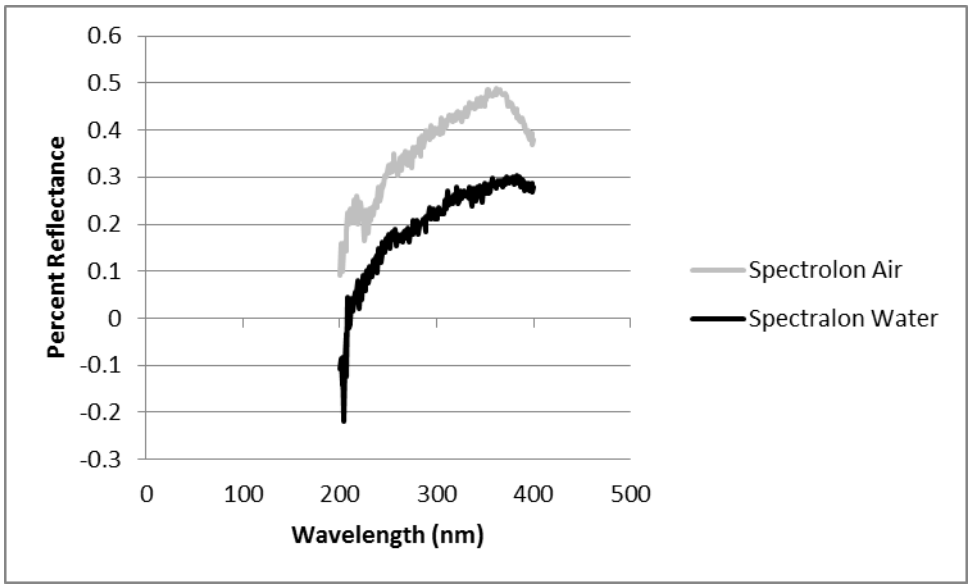

Figure 16: Spectralon® reflectance at 60 degrees

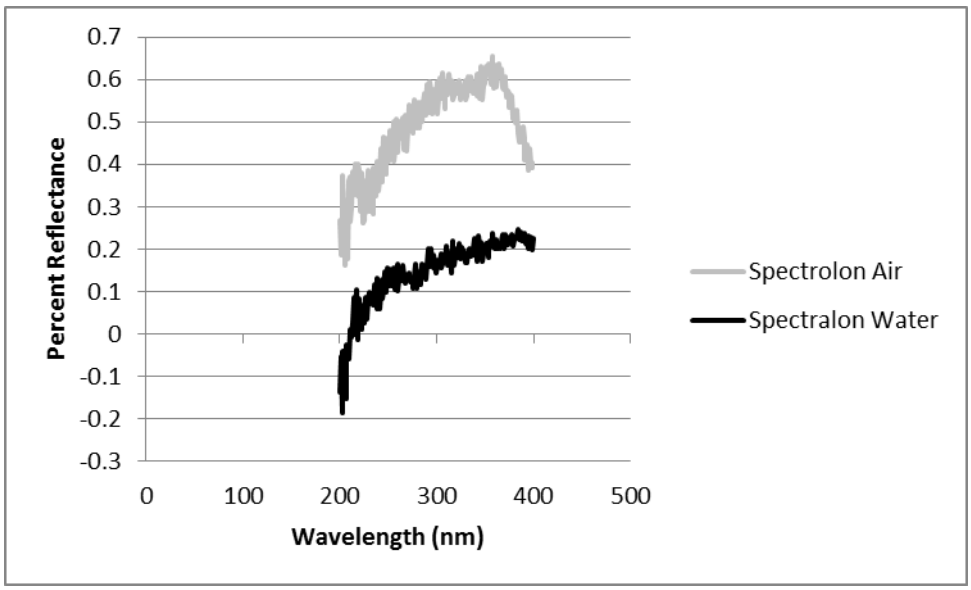

Figure 17: Spectralon® reflectance at 70 degrees

To provide a more representative comparison between the characteristics of Spectralon® in air and water, Snell's law should be applied. Snell's law is defined as:

$$n_1 \sin\Theta_1 = n_2 \sin\Theta_2$$

where: n_1 = the index of refraction of the incident medium

n_2 = the index of refraction of the refraction medium

Θ_1 = the angle of incidence

Θ_2 = the angle of refraction

As shown in Figures 18 and 19, the conclusions still hold with adjusting the different angles of comparison using Snell's law. Upon calculating the difference between air and water, the more representative comparison for the reflectance of Spectralon® is as follows:

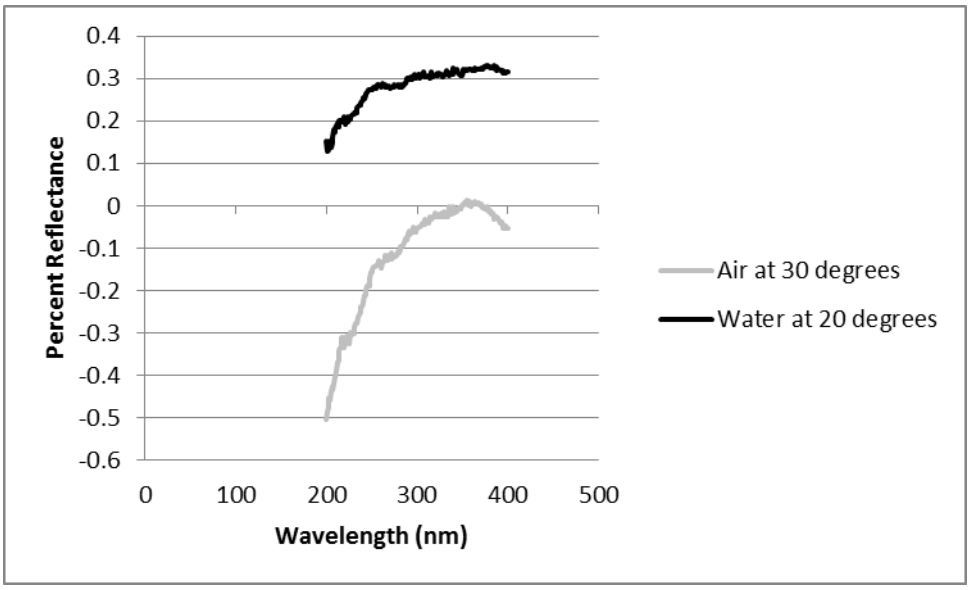

Figure 18: Spectralon® reflectance using Snell's law (1/2)

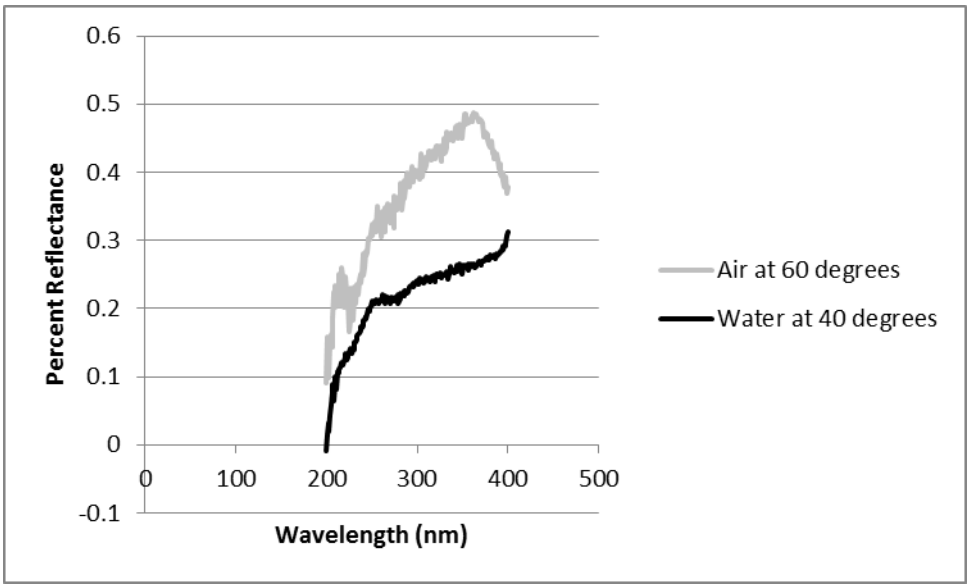

Figure 19: Spectralon® reflectance using Snell's law (2/2)

In addition to the Spectralon® being analyzed by the CARY, some possible materials to build the apparatus for the DNA destruction and hydroxyl radical production experiments were also tested. The two materials that were tested as possible materials for these test cells were stainless steel and aluminum. The plots of the reflectance for these materials may be found in the appendix. These plots indicated that reflectance had a strong dependence on wavelength. The data suggested the shorter wavelengths had less reflectance. This information was not only useful for attempting to find the best material for each application, but it also could be very useful for building the prediction model. There were some key differences in how aluminum acted in air versus water when compared to stainless steel. Since the wavelength range being studied in this research effort was from 240 nm to 270 nm, the comparison of differences was focused at 250 nm. For instance, at 20 degrees aluminum and stainless steel in water has approximately the same reflectance, which was about 35 percent. However, stainless steel at 250 nm and 20 degrees in water had only about a six percent reflectance, while it had about a 20 percent reflectance in air. Reflectance in water begins to become higher than in air for aluminum

up to 40 degrees, while reflectance for stainless steel was more reflective in water than in air through 60 degrees. At 70 degrees reflectance of aluminum in air increased up to around 70 percent, while reflectance in water only increased to about 40 percent. The reflectance of stainless steel in water at 70 degrees remained around 20 percent, while in air it increased to approximately 30 percent. Based upon the plots in the appendix, aluminum appeared to have a substantially higher reflectance. However, it is important to note that the sample of aluminum that was analyzed was polished and represented a best case scenario. When aluminum is exposed to water it has a tendency to oxidize, which will reduces the amount of reflectance it produces. Stainless steel does not oxidize nearly as rapidly as aluminum and was expected to have a higher reflectance over time. In order to make a decision about which material would make the most sense for future design considerations, a further analysis will likely be needed.

UV LED Power Output in Air

The air measurements were collected over a series of weeks, but the calibration and control mechanisms described in Chapter III were always implemented. Various plots were created from the different UV LEDs, but a few representative ones are as follows (the remaining plots are in the Appendix).

Figure 18 show the different characteristic wavelengths for the UV LEDs that were studied in this research effort. The 240 nm UV LED was centered around 245 nm, the 265 nm UV LED was centered around 267, and the 270 nm was centered a 270 nm.

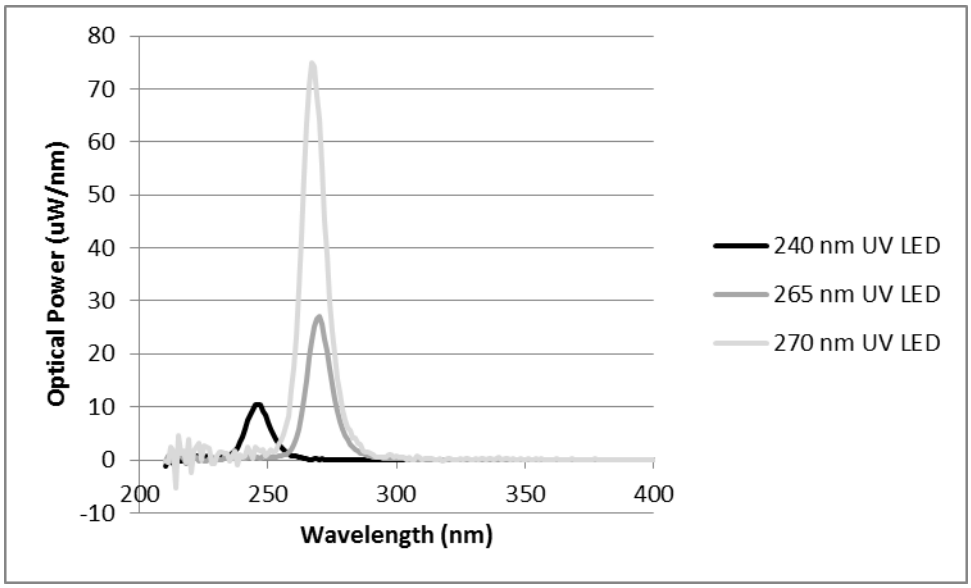

Figure 20. Characteristic Wavelengths Plot

Very little variation existed in the characteristic wavelength for the multiple UV LEDs that were analyzed. Table 1 shows the mean wavelength for the various UV LEDs that were evaluated. F146, F147, and H610 were all 270 nm UV LEDs with the characteristic wavelength 270 nm. D45 was a 240 nm UV LED with a characteristic wavelength of 245 nm. Further as this table shows, the measurements of the center wavelength were consistent whether the UV LED was driven continuously or pulsed at 9.1 Hz with 10, 20, or 30 percent duty cycle.

Table 1: Characteristic wavelengths (λ) for continuously driven and UV LEDs pulsed a 10, 20, and 30 percent duty cycle

S/N	Cont Peak λ (nm)	P10 Peak λ (nm)	P20 Peak λ (nm)	P30 Peak λ (nm)
F147	270.0	270.2	269.8	270.0
D45	246.3	245.0	245.0	245.1
F146	269.8	270.2	270.0	270.0
H610	270.2	270.5	270.2	270.0

Figure 19 indicates that the relationship between current input and power output is linear. This linear relationship is consistent with the UV LED data, indicates that the UV LEDs behave consistently with more established visible light emitting diodes. This relationship held whether the

UV LEDs were new or older since H610 was a 270 nm UV LED with approximately 75 hours of use, while the F146 and F147 are both new 270 nm UV LEDs.

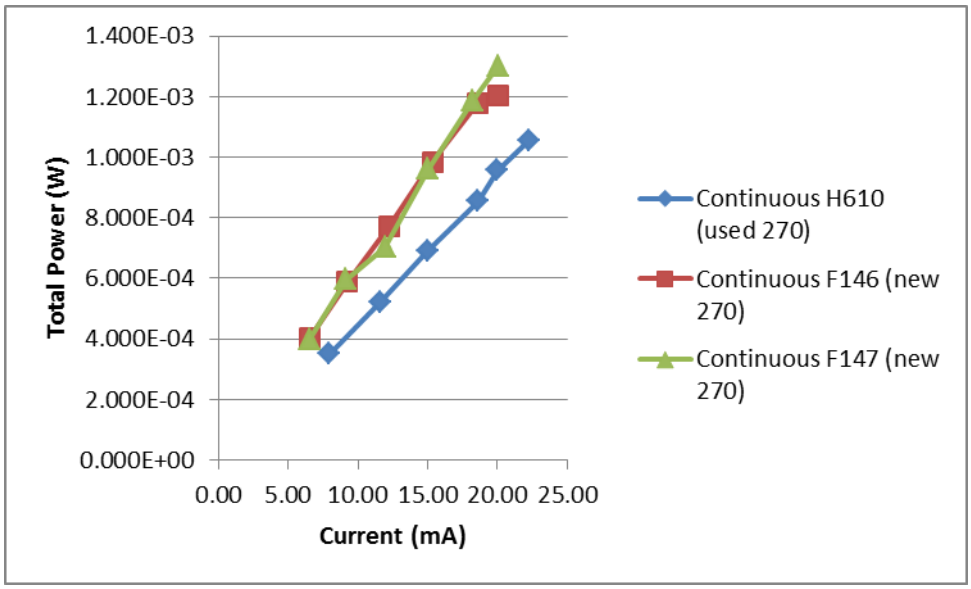

Figure 21: Linear correlation between current and otpical power

To analyze how a 10 percent duty cycle compared to a 100 percent duty cycle another plot was created. Figure 18 is a plot of a new 240 nm and a new 270 nm UV LED that compares power measured from a continuously driven UV LED and the data acquired by measuring the optical power output of an UV LED when driven at a 10 percent duty cycle after this data was multiplied by a factor of ten . As shown, the data for the D45 UV LED was very consistent when driven continuously or 10 times the optical power measured for a 0.1 duty cycle. The data for the F146 diode was slightly lower for the compensated 0.1 duty cycle than the continuously driven F146 diode.

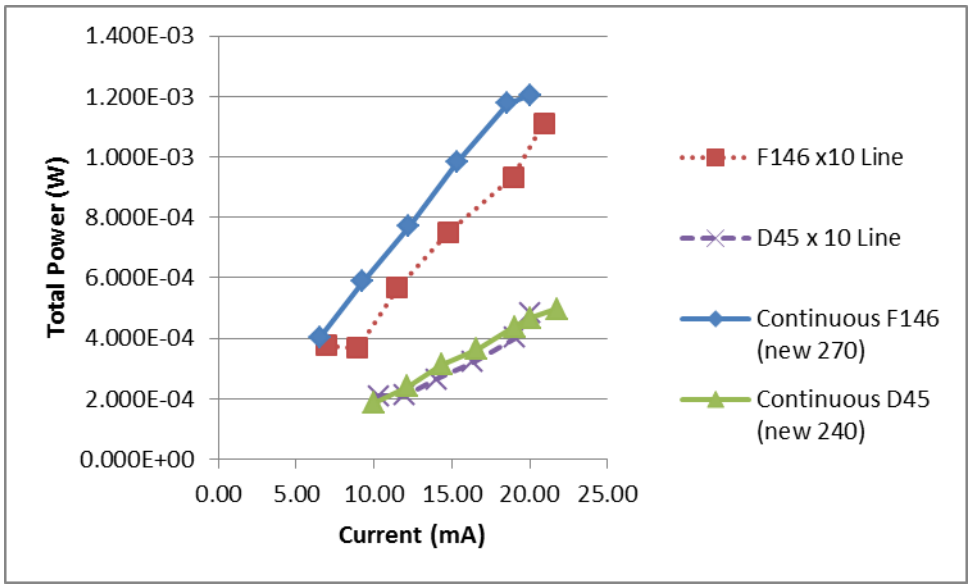

Figure 22: Comparison for continuous and 10 percent duty cycle

Figures 21 through 24 indicate that there is a fairly predictable relationship between the pulse times. The x2 and x3 lines correspond almost identically with the measured 20 percent and 30 percent duty cycle pulses. Measurements indicated this was a much more predictable relationship when the UV LEDs were new. When the UV LEDs had been used for several hours the measured and predicted data did not align as closely, particularly for low current values. The misalignment for low current values might have been due to shifts in the voltage threshold for the UV LEDs, indicating that the turn on voltage may have been higher for low duty cycles. The other important piece to recognize in these plots is the relationship seemed to be clear for both wavelength UV LEDs.

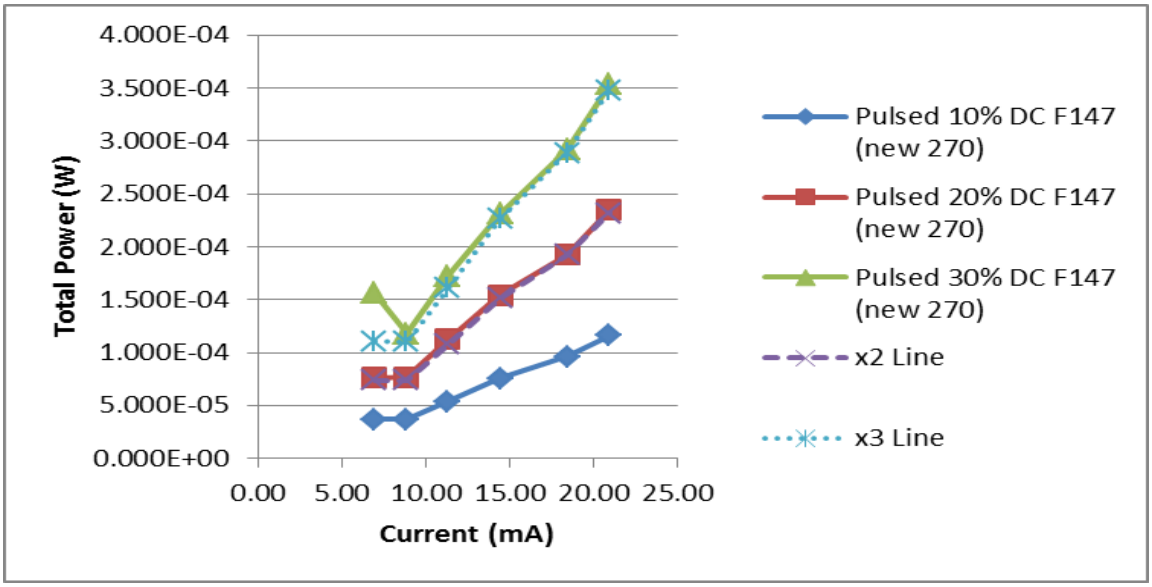

Figure 23: Correlation between various pulses (1/4)

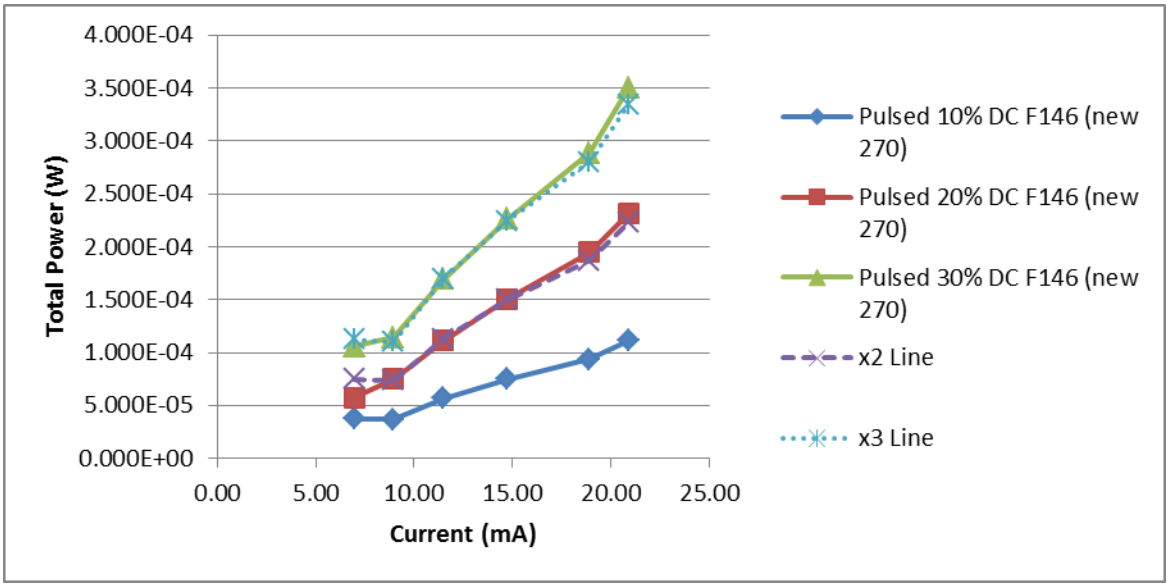

Figure 24: Correlation between various pulses (2/4)

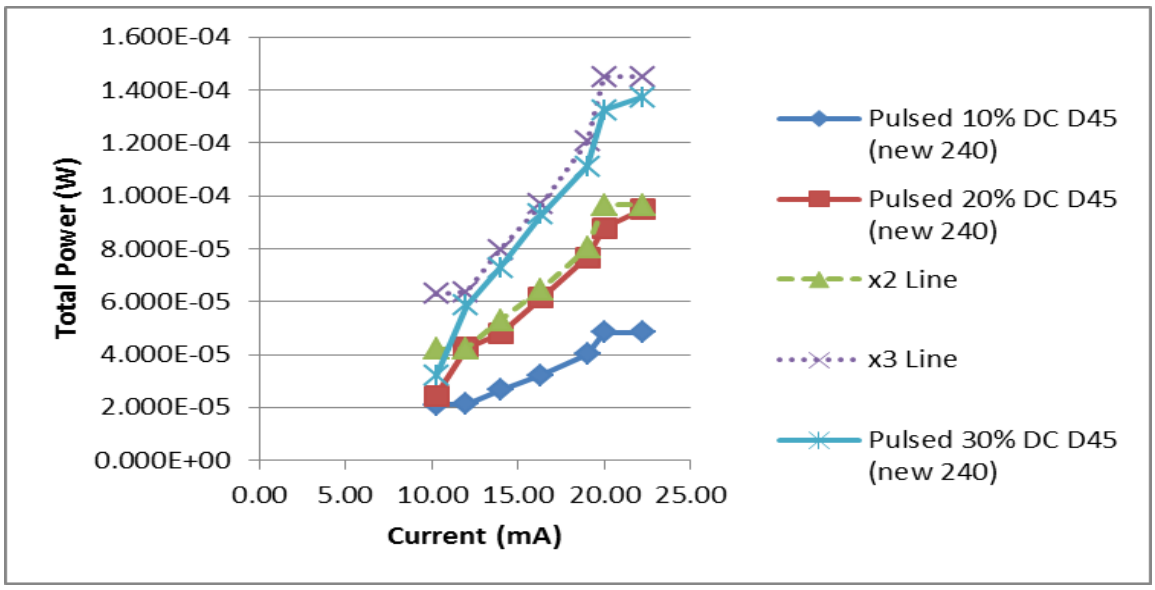

Figure 25: Correlation between various pulses (3/4)

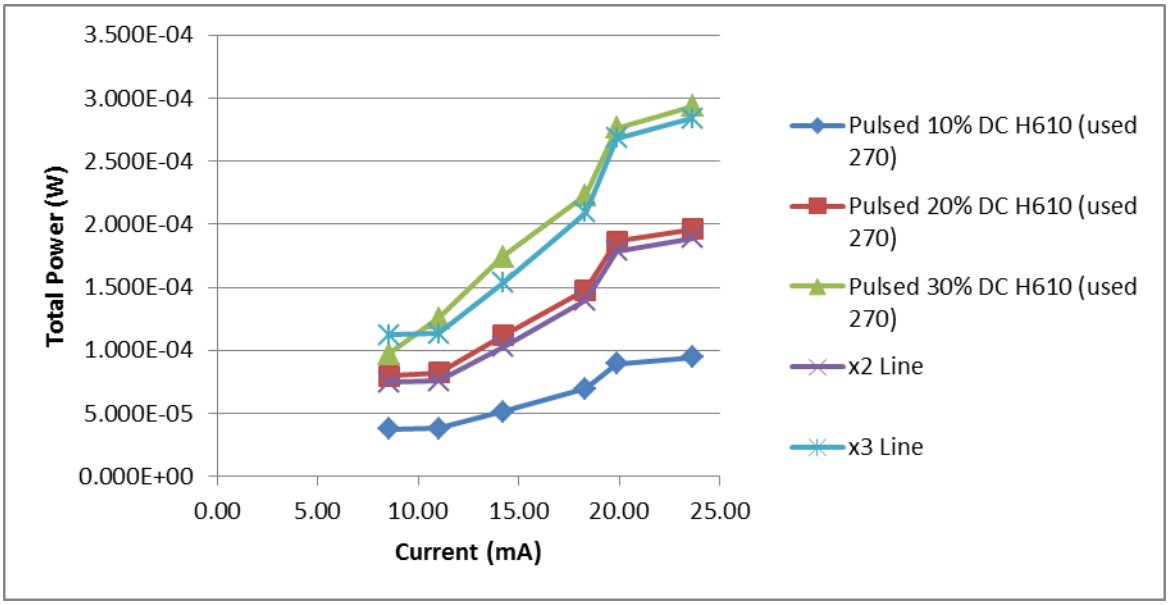

Figure 26: Correlation between various pulses (4/4)

It should also be noted that while Figures 21 through 24 show current on the x axis, these current values could not be accurately measured with the available equipment. The oscilloscope could be used to show the trace and measure a voltage drop across a known resistance in line with the UV LED, but the trace was noisy and measurement would have been very imprecise. Therfore,

Microsoft Excel was used to fit an exponential curve to predict the current as a function of voltage for each UV LED. This equation was then applied to the input voltage value during the pulse conditions to provide an estimate of current The following table outlines these estimates and their respective correlation coefficients for the UV LEDs that are analyzed in Figures 21 through 24.

Table 2: Parameter estimates for Figures 21 through 24

S/N	Equation	R^2
F147	$y=0.0324e^{0.9761x}$	0.988
D45	$y=0.1366e^{0.6172x}$	0.9949
F146	$y=0.0287e^{0.9986x}$	0.986
H610	$y=0.0316e^{1.0181x}$	0.9817

To further characterize the pulsed and continuous wave similarities in ouput optical power, a plot of a new 240 nm and 270 nm UV LEDs under continuous and a 10 percent duty cycle conditions were analyzed. Figure 25 illustrates this relationship.

To calculate the efficiency of the different UV LEDs, a ratio of the optical power and the electrical power was taken. Table 3 indicates what the efficiencies were at 20 mA for each UV LED.

$$\eta = \frac{Power\ Output}{Current}$$

Table 3: UV LED Efficiencies

H610 (used 270)	**Efficiency**		**F146 (new 270)**	**Efficiency**
Continuous	4.79%		Continuous	6.01%
10% Pulsed	0.45%		10% Pulsed	0.53%
20% Pulsed	0.94%		20% Pulsed	1.11%
30% Pulsed	1.39%		30% Pulsed	1.67%
F147 (new 270)	**Efficiency**		**D45 (new 240)**	**Efficiency**

Continuous	6.49%		Continuous	2.33%
10% Pulsed	0.55%		10% Pulsed	0.24%
20% Pulsed	1.12%		20% Pulsed	0.44%
30% Pulsed	1.69%		30% Pulsed	0.66%

One further piece of analysis determined what the spread over the various wavelengths looked like when comparing continuous and pulsed UV LEDs. The follwing plot in Figure 26 illustrates the spectral distribution of energy output from a sample UV LED under continuously driven and a 10% pulsed condition. Note that the power for the 10% pulsed condition was multiplied by 10 to provide comparable spectra. Another important point to note about the figure below is the UV LED being analyzed here is a 265 nm UV LED. The difference between the pulsed and continuous is not as well understood for this wavelength and therefore the difference in this normalized plot is not as easily explained.

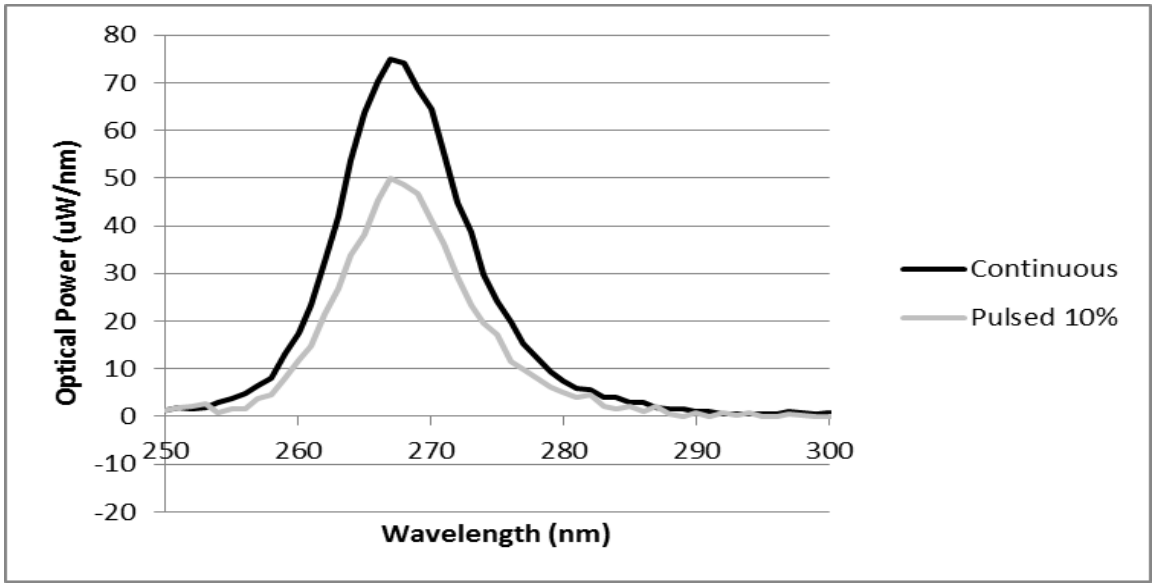

Figure 27: Normalized Integrated Power comparison plot for 270 nm UV LED (1/2)

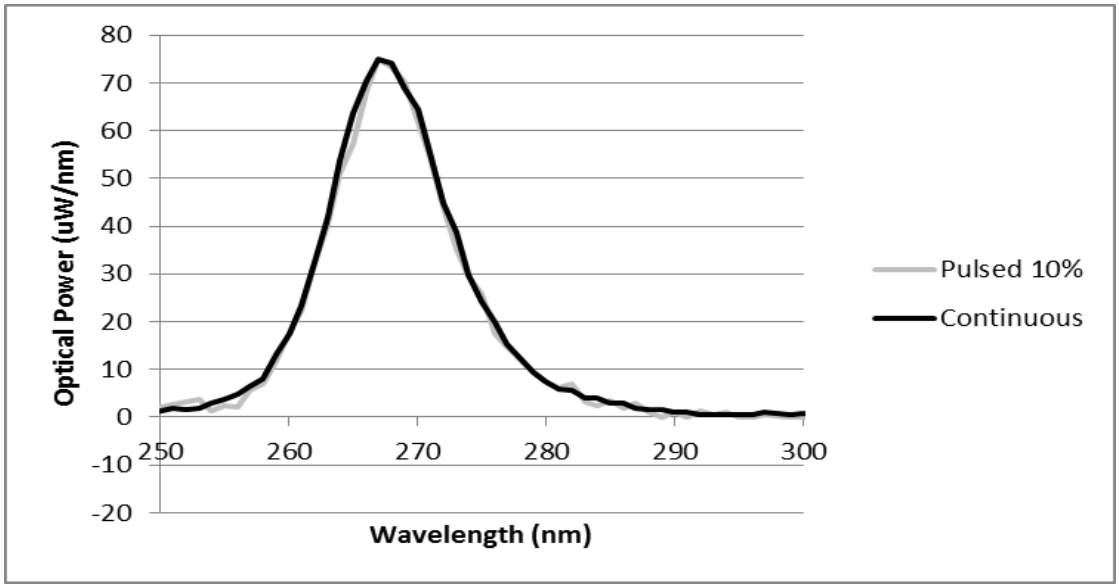

Figure 28: Normalized Integrated Power comparison plot for 270 nm UV LED (2/2)

UV LED Power Output in Water

The water measurements were more challenging and time consuming to obtain. Unfortunately, due to technical difficulties and time constraints, the water measurements were unable to be collected. The original apparatus provided by Labsphere for these measurements included an electronic shutter at the top of the integrating sphere to protect the fiber optic cable from UV exposure between measurements. Unfortunately, the electronic shutter could not be immersed in water and required the maintenance of an air gap between the water in the integrating sphere and the fiber optic cable. Measurements attempted with this apparatus failed to provide the spectral radiometer with sufficient energy to permit a measurement. As it was hypothesized that the air gap was resulting in excessive energy loss, a new adapter was procured from the manufacturer of the apparatus which permitted the fiber optic cable to be attached directly to the sphere and to fully immerse the sphere in water, eliminating the air gap.

Measurement was again attempted with the modified apparatus. It was found that the sensor received adequate energy to permit a measurement. However, the energy levels in the water-filled

sphere was significantly lower than for the air measurements, requiring integration times that were up to 150 times longer than were required for the air measurements. Further, when the measurements were obtained with these long integration times, the sensor obtained a spectral signature in raw pixel values that were similar to those obtained in air. Unfortunately, when the calibration was applied to convert these raw pixel values to power, the resulting spectral signal was noisy and the signal to noise ratio to be too small to be useful.

It was also observed that the water level steadily declined over several days. This was likely due to evaporation and potentially some absorption into the Spectralon® since it is a porous material. There was also a noticeable amount of oxidation of the bolts for the sphere base and the taps for the UV LED plate, which had originally been assumed to be made of stainless steel.

The chiller was an issue because the cooling occurred for too long. For instance, if the temperature was supposed to be maintained at 22 degrees Celsius, at 23 degrees Celsius the chiller would turn the fan on and cool the UV LED down as far as 17 degrees Celsius. This large difference in temperature and uncontrollable switch created some inaccuracy and inconsistency. Unfortunately, the chiller did not work properly due to the inadequate design of the connections for the chiller from Labsphere®. The chiller was connected to the UV LED chamber by two small wires, which provided the temperature readings to the Illumia Pro software. However, the metal plate that fit over the UV LED made contact with other metal, which caused the circuit to short-circuit. To resolve this issue a small piece of shrink wrap (a small plastic bag) was placed between the two metal surfaces to alleviate the short-circuit issue. This caused the chiller to become confused about the readings and large fluctuations in temperature were experienced, which defeated the purpose of using the chiller.

The DAQ being limited to 10 volts was another limitation. The driver boards were designed to be able to drive 24 volts because it was anticipated that higher voltage would be needed for some UV

LEDs in the AOP and disinfection projects. Since the DAQ was limited to 10 volts, a multiplier had to be installed on the board that drove the disinfection project. The signal to noise ratio for the power measurements for the sphere in water were much more of an issue than the sphere in air. A few possible explanations of why there was such a large difference occurred could be the air interface before the spectrometer could have seen the measurements because the shutter could not get wet or the fact that the lamp was calibrated in air instead of water. The accuracy of the measurements may have been slightly impacted because of this and the power would have certainly been different for water because the measurements took so long to be captured. The air measurements took approximately 30 seconds per capture point, while the water measurements took close to 45 minutes per capture point. The average life of the UV LED, according to the manufacturer's data, was approximately 150 hours. While the degradation curve is currently not well understood, a large amount of degradation was assumed to be occurring in the first 50 hours. The measurements provided by the manufacturer in the technical data for the UV LEDs were often quite different than the data the students measured in this research project. For instance, the power measurements according to the integrating sphere in air were approximately 50% more than what was claimed by the manufacturer. The UV LED's performance in water was expected to be better, which would imply the data provided must be after so many hours of burning. However, the data provided did create a starting point for determining how long to run an experiment for the disinfection project.

In addition, there were also multiple assumptions that had to be made in order to proceed with the experiments. The key assumptions made were that the DASYLAB signal stayed consistent for all of the experiments, the reverse osmosis water used was very similar to distilled water, the oxidation of the metal components in the water did not create a major change in the characteristics of the water, switching boards from the air measurements to the water measurements did not create a major impact

on the accuracy of the measurements, the difference between the UV LED measurements are attributed to the differences in them from the manufacturer and from the amount of time burning for testing, the change in water level due to evaporation and absorption into the Spectralon® does not create a major impact in the accuracy of the measurements, and the calibration properly accounted for the material inside of the sphere for the power measurements.

While every software program has its limitations and tolerance for executing code, the expectation with the measured data was that the amount of difference did not greatly impact the results that were collected. There certainly are chemical differences between water that is considered "distilled" and water that is from a reverse osmosis system. The amount of filtration the reverse osmosis system is based on what is desired to be not in the water. The measurements for this research effort assumed there was no difference in these two types of water, which could make a slight difference in the performance of the UV LED. Furthermore, there was oxidation of the metal components connecting all of the necessary items to conduct the experiment. This oxidation may have altered the chemical properties of the water, but the data again assumed the changes in the water's properties. Another consideration that must be considered with respect to the water was the evaporation and the absorption into the porous Spectralon®, which caused the water level inside of the fish tank to continually be reduced. The noticeably different performance parameters in the UV LEDs also introduced some uncertainty in the measurements taken for the different research projects encompassed. The calibration process should have introduced minimal uncertainty since it was consistently performed in the same manner for all measurements taken. Switching boards should also have introduced very little uncertainty since the boards are very similar in nature.

V. Conclusion

This research effort characterized optical power for short wavelength UV LEDs. A theorized linear correlation between current and power for both air and water was utilized, however, it could not be proven due to the inability to collect accurate water measurements. Unfortunately, the measurements taken using the air integrating sphere was unable to provide the supporting data to prove this theory. In addition, the performance for the various UV LEDs were analyzed.

This research studied how the performance was different for a new and used UV LEDs. The used UV LEDs were near the manufacturer's estimated end of life. As one would expect, the used UV LED provided less optical power than a new UV LED. Another interesting finding is that the ability to predict the effect of duty cycles on UV LEDs appears to change over time, with power output varying only as a function of the on-time for new LEDs but with aged LEDs providing less power when pulsed at shorter durations when correcting for on-time.

A study was conducted to explore how the reflectance of Spectralon® changes when it is immersed in water. Spectralon®'s published reflectivity in air is 99.99 percent, but there is no published reflectivity for it in water. The CARY 5000 photospectrometer used in this research effort was not designed to conduct this type of experiment, however, to the author's knowledge no other instrument has been designed for this purpose either. For the Spectralon® to be submerged in water, a sample holder had to be created to fit in the CARY 5000. This sample holder changed the way the background correction needed to be taken, which introduced some error. The plots comparing the differences in Spectralon®'s behavior in air and water demonstrate that this procedure introduced error as it resulted in negative reflectivity values. However, the results do indicate that the reflectivity of spectralong becomes less diffuse in water and the reflectivity of this material is reduced for very short

wavelength UV LEDs. This indicates that this material is not as ideal for UV measurements in water as it is for visible light measurements in air. This is particularly true for wavelengths less than 250 nm.

The differences in power produced for the different wavelengths, as well as voltage and current relationships, were also studied. There appeared to be a relatively large variation between the manufacturer's claims in their specifications for the UV LEDs and the experimental results. A few examples include the input voltage required to turn on the UV LED and the total output optical power. There was up to a 50 percent difference in optical power between experimental results and manufacturer specifications for one of the UV LEDs with the measured values exceeding the manufacturer's claimed values. Additionally, even the manufacturer identified large variations between UV LEDs that are supposed to be virtually identical. For instance, one would expect that for two different 270 nm UV LEDs from the same batch and manufacturer, would have similar specifications. However, there was a noticeable difference in required input voltage to obtain the desired 20 mA current, within the manufacturer's specifications and the measured values.

In summary, this thesis has addressed methods to quantify the optical performance of UV LEDs. As these devices have applicability in sensing of organic compounds and purifying water, it is hoped that these methods and findings inform future research activities, helping to transition these devices into environmental health applications where they are beneficial.

Appendix

Continuous DASYLAB program

- Time base: this provides the software a clock to be able to sync the data that is being collected as the program runs
- Formula interpreter x2: one is intended to calculate the current (using V=IR) and the other is intended to create a safety to turn the program off when the current became "too high" (but the program kept shutting down so currently it just the program just bypasses this one by inputting a 1)
- Digital meter: digitally displays the voltage, temperature, and the voltage drop while the program is running
- Plot: this plot is intended to illustrate the input voltage and the calculated current for each UV LED (currently setup for 7 UV LEDs)
- Write: records input voltage, temperature, and voltage drop in a text file

Pulsed program

- Signal generator: allows the user to select different kinds of wave forms (rectangular, triangular, etc.) and allows the user to input a frequency, voltage, offset, and duty cycle
- Plot: serves to let the user know the UV LED has started pulsing (buffer time takes several seconds) and displays what the shape of the pulse signal looks like

The reflectance measurements for aluminum and stainless steel were obtained in a very similar manner as the Spectralon® samples. Similar to the mirror, spacers were necessary to hold the samples of aluminum and stainless steel as vertical as possible to minimize the effect of reflection in the z-axis direction.

Reflectance for Aluminum

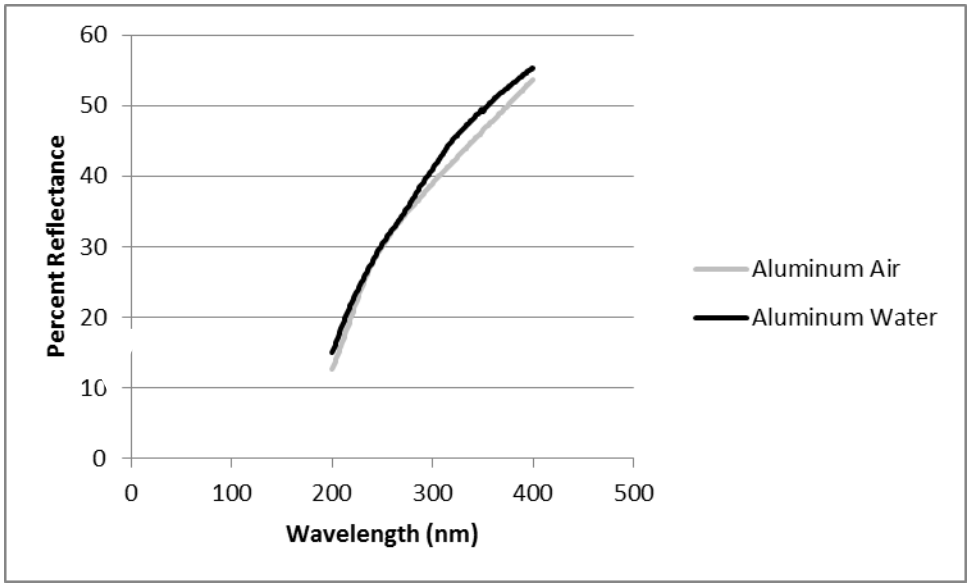

Figure A-1: Reflectance for aluminum in air versus water at 20 degrees

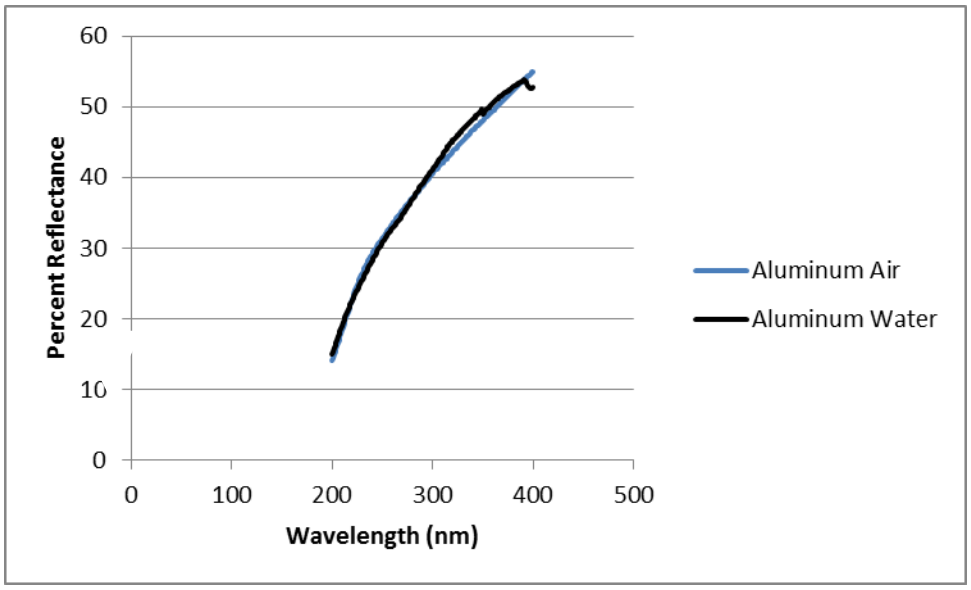

Figure A-2: Reflectance for aluminum in air versus water at 30 degrees

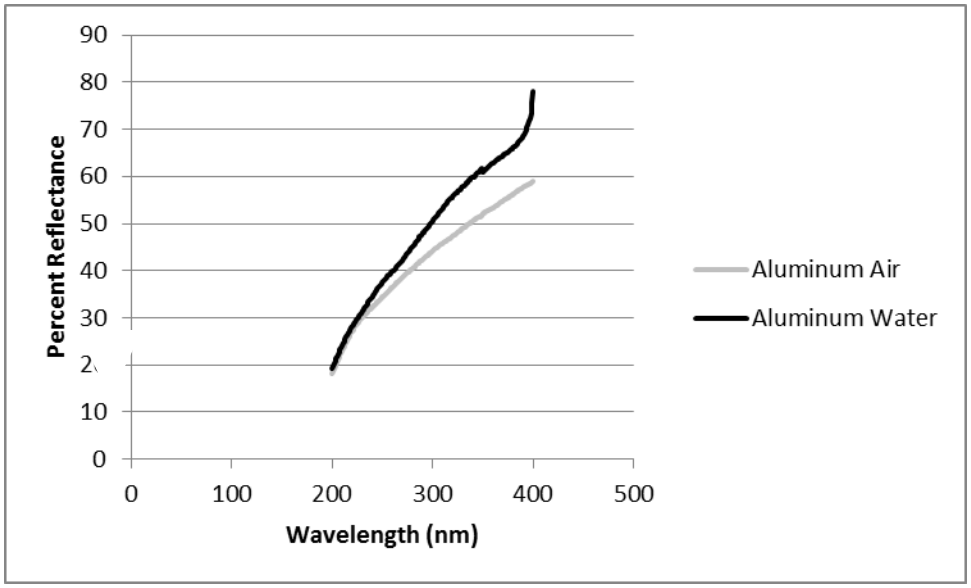

Figure A-3: Reflectance for aluminum in air versus water at 40 degrees

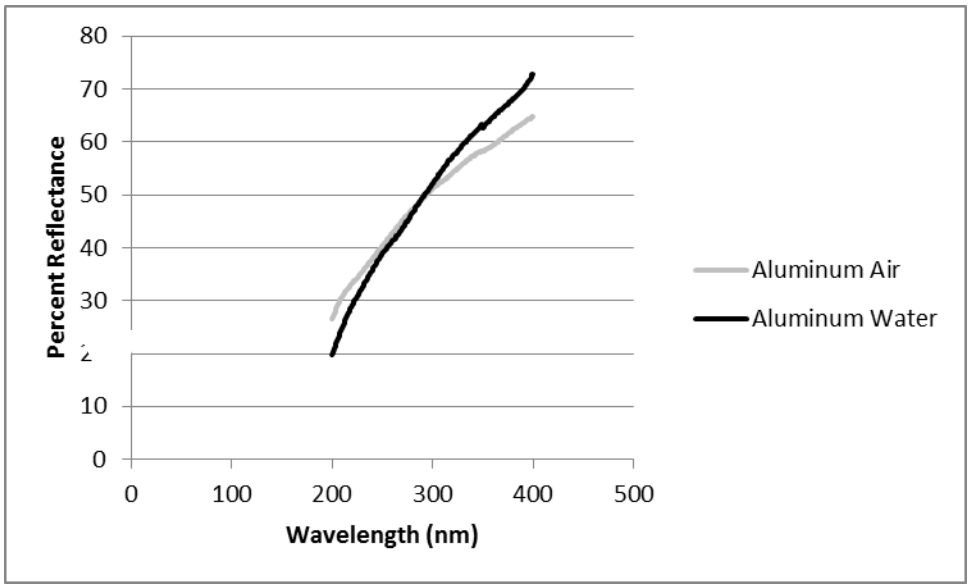

Figure A-4: Reflectance for aluminum in air versus water at 50 degrees

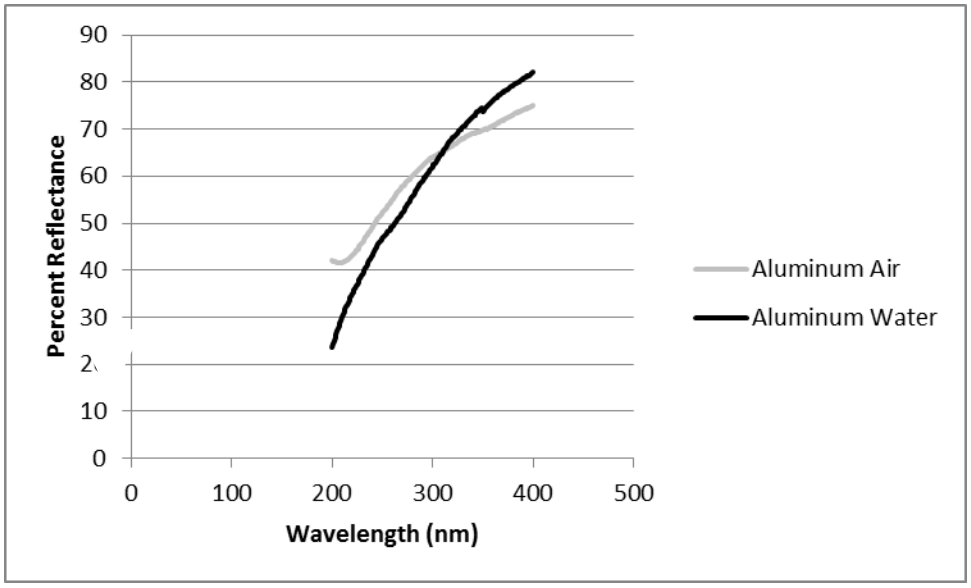

Figure A-5: Reflectance for aluminum in air versus water at 60 degrees

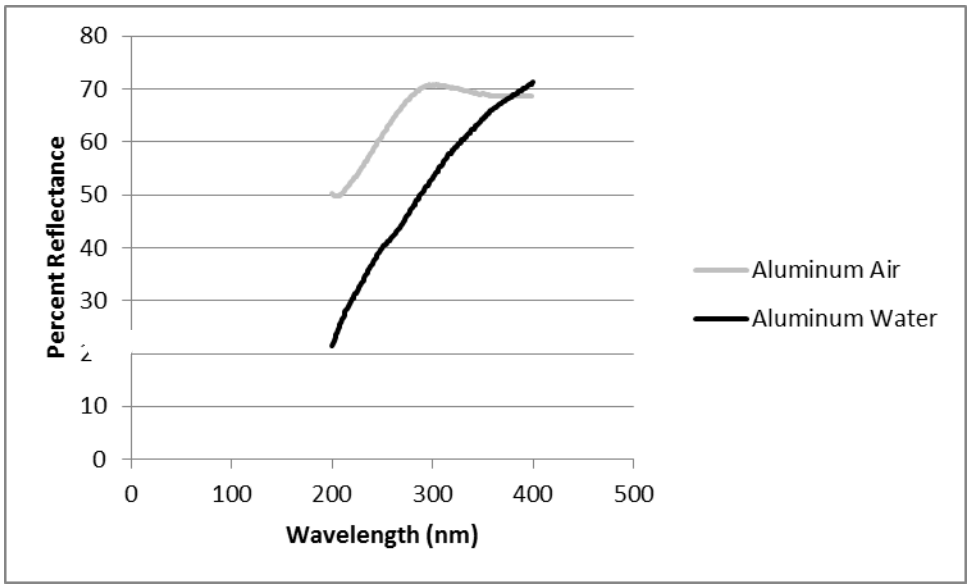

Figure A-6: Reflectance for aluminum in air versus water at 70 degrees

Reflectance for Stainless Steel (to explain apparatus for other 2 projects)

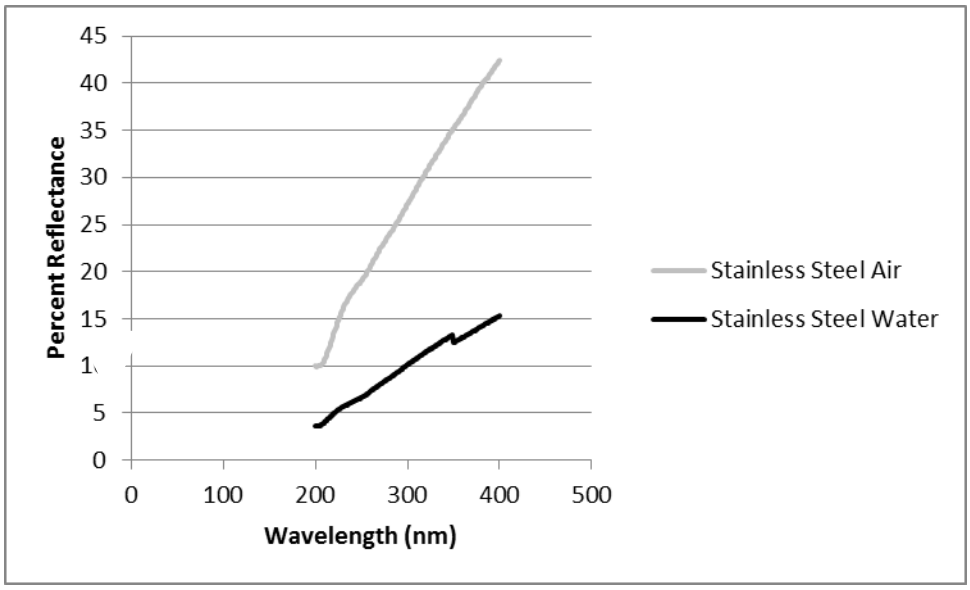

Figure A-7: Reflectance for stainless steel in air versus water at 20 degrees

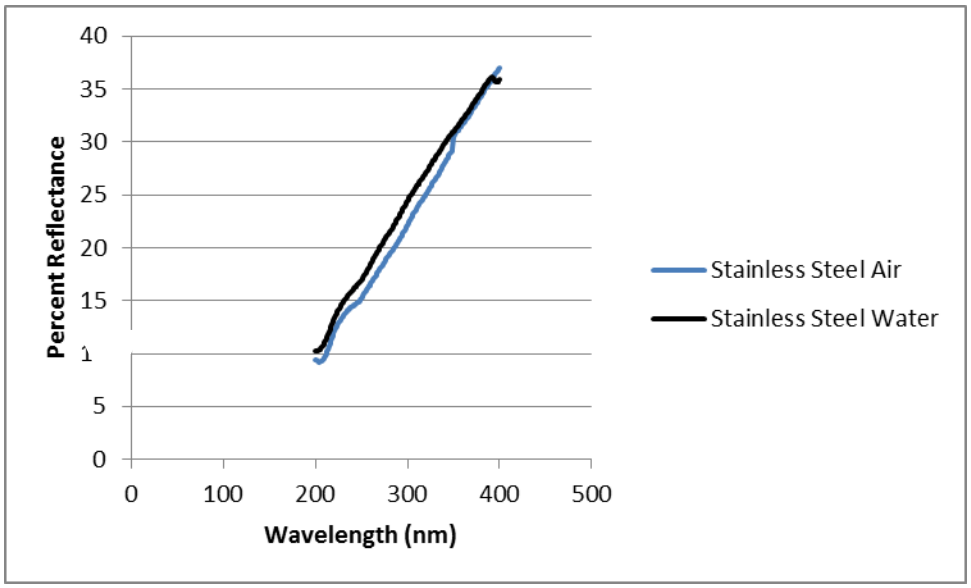

Figure A-8: Reflectance for stainless steel in air versus water at 30 degrees

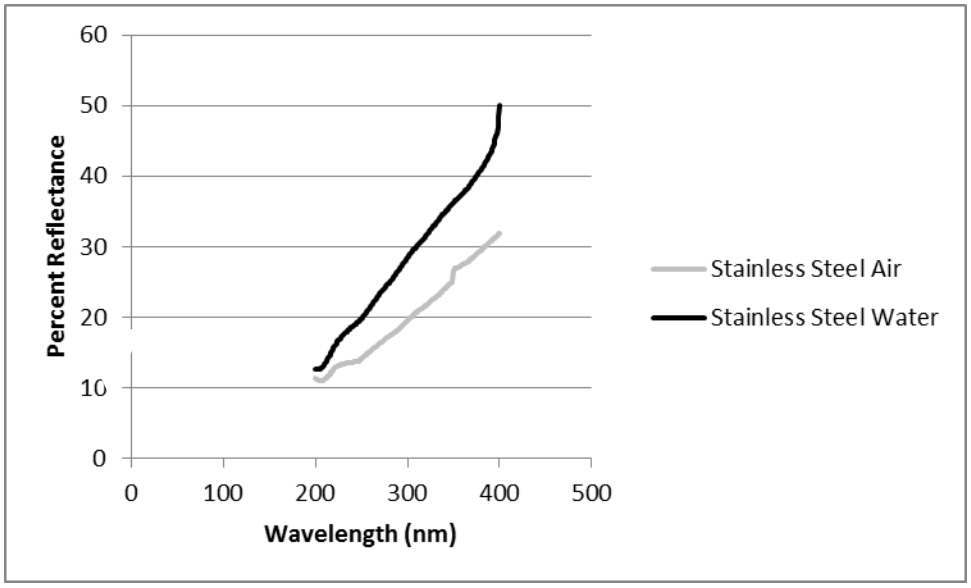

Figure A-9: Reflectance for stainless steel in air versus water at 40 degrees

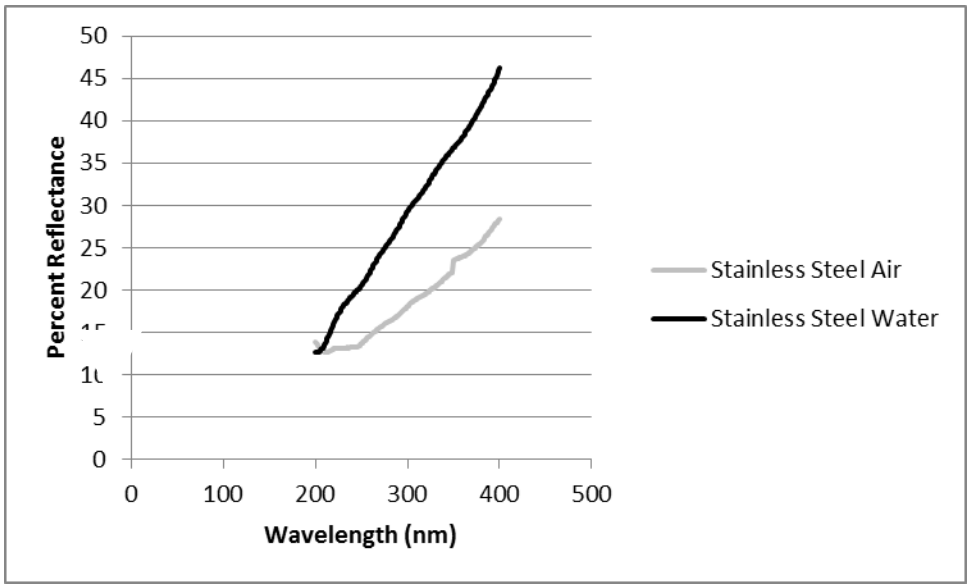

Figure A-10: Reflectance for stainless steel in air versus water at 50 degrees

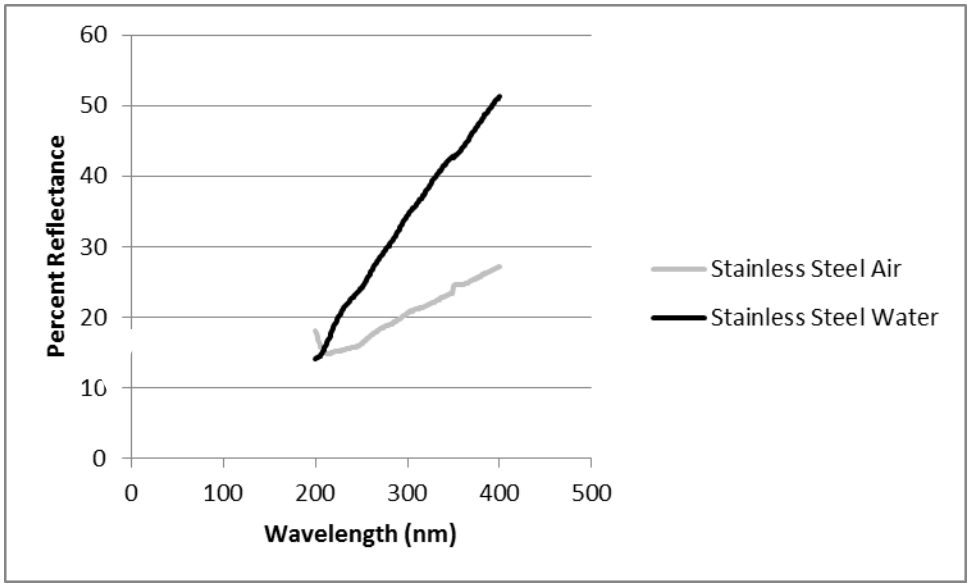

Figure A-11: Reflectance for stainless steel in air versus water at 60 degrees

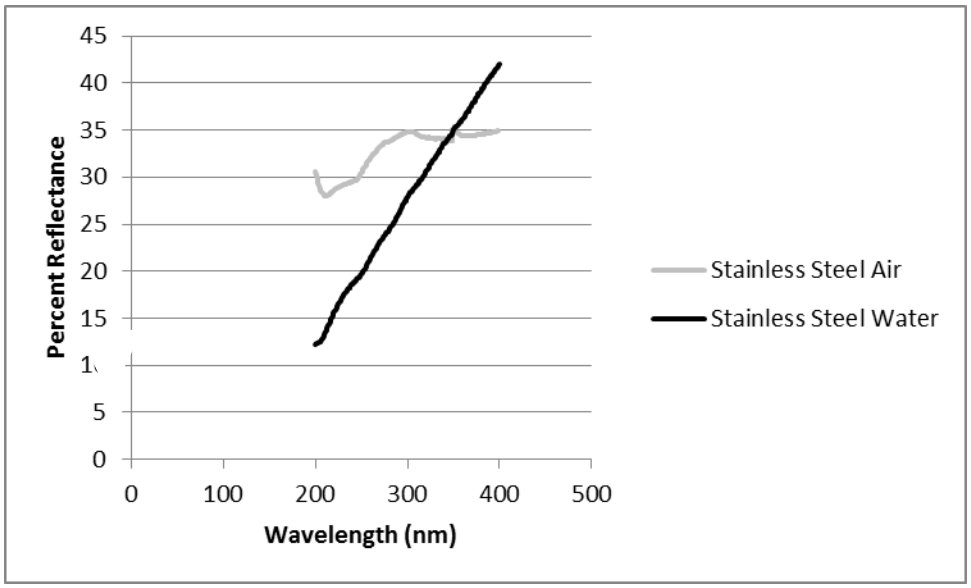

Figure A-12: Reflectance for stainless steel in air versus water at 70 degrees

Remaining Output Power Graphs:

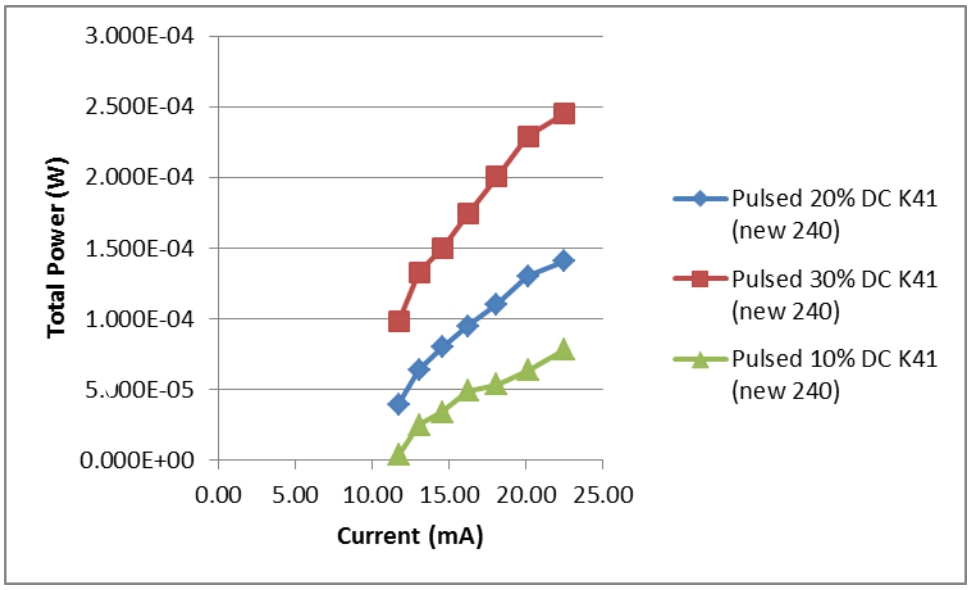

Figure A-13: Correlation between various pulses

Since current could not be measured directly like in the continuous configuration, Microsoft Excel was used to fit an exponential curve to predict the current for each UV LED. The following table outlines these estimates:

Table A-1: Parameter estimates for Fig A-13

S/N	Equation	R^2
K41	$y=0.5652e^{0.4333x}$	0.9839

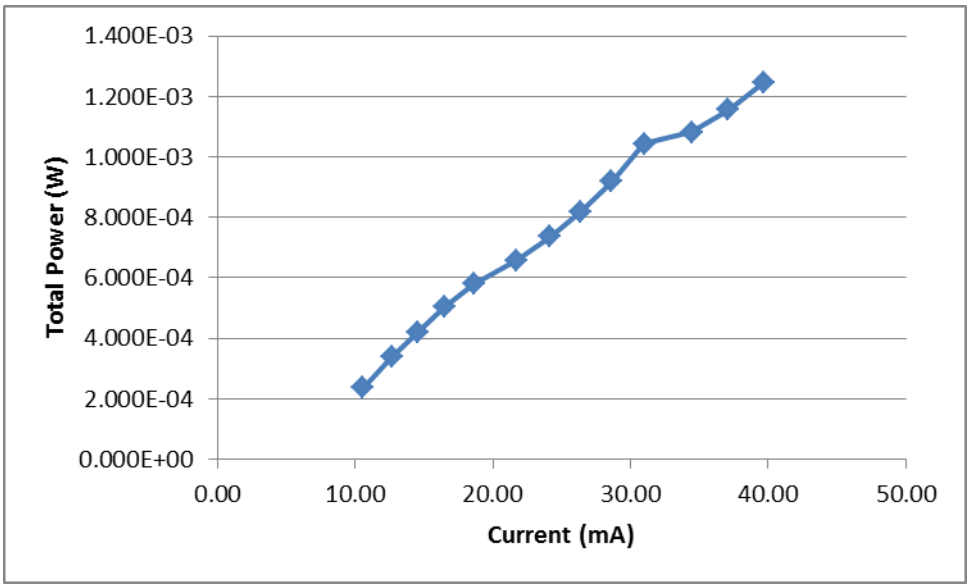

Figure A-14: Correlation between total power and current for K41 (new 240)

Bibliography

Agilent CARY 4000_6000i, 2011.
http://global-oceans.org/site/wp-content/uploads/2013/05/Agilent%20Cary%204000_6000i.pdf

Arroyo Instruments, 2014.

http://www.arroyoinstruments.com/categories/temperature-controllers

CARY 4000_5000_6000i, 2011.
http://mmrc.caltech.edu/Cary%20UV-Vis%20Int.Sphere/manuals/4000_5000_6000i_external_dra.pdf
Cree, 2014. http://www.cree.com/LED-Chips-and-Materials/Chips/Chips/Direct-Attach/DA1000-

LED

DASYLAB, 2014.

http://www.arroyoinstruments.com/categories/temperature-controllers

Extech Instruments, 2014.

http://www.arroyoinstruments.com/categories/temperature-controllers

High performance AlGaInP visible light-emitting diodes. Appl Phys Lett 1990 57(27):2937-9.

Kuo CP, Fletcher RM, Osentowski TD, Lardizabal MC, Craford MG, Robbins VM.

Labsphere. 2014.
http://www.labsphere.com/products/reflectance-standards-and-targets/spectralon-reflectance-standards/default.aspx

http://www.labsphere.com/products/spheres-and-components/general-purpose-spheres/radiometer-photometer.aspx

http://www.labsphere.com/products/light-measurement-systems/illumia-light-measurement-products/default.aspx

Lenk, Ron, Lenk, Carol. "Practical Lighting Design with LEDs". *The Institute of Electrical and Electronics Engineers, Inc.*, 2010.

Measurement Computing 2014.

http://www.arroyoinstruments.com/categories/temperature-controllers

Moller, W. "Degradation of the diffuse reflectance of Spectralon® under low-level irradiation". *Institute of Physics Publications*, 2003.

Oak Ridge National Laboratory. 2014. http://web.ornl.gov/~odg/spectrophotometer.html
Ocean Optics, 2014.
http://www.arroyoinstruments.com/categories/temperature-controllers

OWON, 2014.
http://www.arroyoinstruments.com/categories/temperature-controllers

Ping-Shine, S. "Ultraviolet characterization of integrating spheres". *Institute of Physics Publications*,2003.

Sensor Electronics Technology, Incorporated, 2014. http://www.s-et.com/

Phytosafe. 2013. http://www.phytosafe.com/analytics/uv-detection.php

Seton Hall University. 2014. http://hplc.chem.shu.edu/NEW/HPLC_Book/Detectors/det_uv.html

US Peroxide, 2012.http://h2o2.com/technical-library/physical-chemical-properties/radiation-properties/default.aspx?pid=65&name=Ultraviolet-Absorption-Spectrum (accessed 17 Jul 12).

Würtele, M.A., Kolbe, T., Lipsz, M., Külberg, A., Weyers, M., Kneissl, M., and Jekel, M., 2011. Application of GaN-based ultraviolet-C light emitting diodes – UV LEDs – for water disinfection. *Water Research* 45, 1481-1489.

REPORT DOCUMENTATION PAGE

Form Approved

1. REPORT DATE *(DD-MM-YYYY)*	**2. REPORT TYPE**	**3. DATES COVERED** *(From – To)*
27-03-20143	Master's Thesis	Oct 2013 – Mar 2014

4. TITLE AND SUBTITLE
Ultraviolet Light Emitting Diode Optical Power Characterization

5a. CONTRACT NUMBER

5b. GRANT NUMBER

5c. PROGRAM ELEMENT NUMBER

6. AUTHOR(S)
Bates, Christopher S., Captain, USAF, BSC

5d. PROJECT NUMBER
13V117

5e. TASK NUMBER

5f. WORK UNIT NUMBER

7. PERFORMING ORGANIZATION NAMES(S) AND ADDRESS(S)
Bates, Christopher S., Captain, USAF, BSC
Air Force Institute of Technology
Graduate School of Engineering and Management (AFIT/ENV)
2950 Hobson Way, Building 640
WPAFB OH 45433-7765

8. PERFORMING ORGANIZATION REPORT NUMBER
AFIT-ENV-14-M-07

9. SPONSORING/MONITORING AGENCY NAME(S) AND ADDRESS(ES)
US Environmental Protection Agency
25 W. Martin Luther King Dr.
Mailstop NG-16
Cincinnati, OH 45268
Matthew Magnuson
(513) 569-7321
Magnuson.Matthew@epa.gov

10. SPONSOR/MONITOR'S ACRONYM(S)
EPA/NHSRC

11. SPONSOR/MONITOR'S REPORT NUMBER(S)

12. DISTRIBUTION/AVAILABILITY STATEMENT
APPROVED FOR PUBLIC RELEASE; DISTRIBUTION UNLIMITED

13. SUPPLEMENTARY NOTES
This material is declared a work of the U.S. Government and is not subject to copyright protection in the United States

14. ABSTRACT
Obtaining a cost effective way to produce safe drinking water is not only a priority of almost every residential community in the United States, but the Department of Defense has a specific interest cutting edge technology in this domain for disinfecting water in a foreign nation during a war campaign. The development of ultraviolet (UV) Light Emitting Diode (LED) technology is a potentially important step towards being able to conduct this kind of disinfection with fewer resources. The traditional UV source in use for disinfection today is the mercury lamp. This UV source requires high amounts of voltage, requires significant periods of time for warming up, and is not typically lightweight enough or versatile enough to be useful in a deployed setting. This project is intended to characterize the optical power for various short wavelength UV LEDs. This optical power is important in determining how much current is needed to deactivate bacteria and other pathogens or to optimize hydroxyl radical production to oxidize compounds in water. The results from this study indicate there is a linear relationship between optical power and current for air measurements. The data collected in this research were applied to characterize the performance of LEDs for the two tandem projects and building a model to optimize the design and performance of UV LED based reactors. Additionally, this research attempted to measure UV LED emission in water. Issues associated with these measurements are discussed.

15. SUBJECT TERMS
Ultraviolet Light Emitting Diode Optical Power Characterization

16. SECURITY CLASSIFICATION OF:			**17. LIMITATION OF ABSTRACT**	**18. NUMBER OF PAGES**	**19a. NAME OF RESPONSIBLE PERSON**
a. REPORT	**b. ABSTRACT**	**c. THIS PAGE**			Michael E. Miller AFIT/ENV
U	U		UU	70	**19b. TELEPHONE NUMBER** *(Include area code)* (937) 255-3636, x 4651 Michael.Miller@afit.edu

Standard Form 298 (Rev. 8-98)

Prescribed by ANSI Std. Z39-18